

# MECH 325

Machine Design

## CSA - OASYS Leveling Mechanism

Project Report



### Group 19

Igal Avimelek, 96149810

Ronny Cravioto-Ross, 60525243

Danny Elizur, 25491721

Junheon Kim, 85203354

Colin Kitts, 49968738

Alexander Koochin, 63039663

Jaden Pereira, 48349799

Stanley Yang, 60773926

Report Submitted: December 6th, 2025

<b>1. INTRODUCTION .....</b>	<b>1</b>
1.1. Summary.....	1
1.2. Client .....	1
<b>2. PURPOSE .....</b>	<b>1</b>
2.1. Scope .....	1
2.2. Functions .....	2
2.3. Design Requirements .....	2
2.4. Evaluation Criteria .....	3
2.5. Key Components.....	3
<b>3. ANALYSIS .....</b>	<b>4</b>
3.1. Assumptions and Simplifications.....	4
3.2. Inputs .....	4
3.3. Materials .....	4
3.4. Lead Screw .....	5
3.5. Stabilizer Beam and Hinge (Including Pin/Bolt Analysis for Hinge).....	7
3.6. Dust Cover.....	9
3.7. Bearings .....	10
3.8. Ball Joint.....	12
<b>4. RESULTS.....</b>	<b>13</b>
4.1. Final Design .....	13
4.2. Power Requirements .....	14
4.3. Safety Factors.....	15
<b>5. CONCLUSIONS AND RECOMMENDATIONS .....</b>	<b>15</b>
5.1. Summary.....	15
5.2. Future Actions .....	15

<b>6. REFERENCES .....</b>	<b>17</b>
6.1. Materials: .....	17
6.2. Lead Screw .....	17
6.3. Dust Cover.....	17
6.4. Bearings .....	17
6.5. Power Requirements .....	17
<b>7. APPENDIX A – CALCULATIONS, DETAILED ANALYSIS.....</b>	<b>18</b>
7.1. Lead Screw .....	18
7.2. Outrigger Beam and Hinge (Including Pin/Bolt Analysis for Hinge).....	31
7.3. Bearings .....	40
7.4. Ball Joint.....	42
<b>8. APPENDIX B – EXTRA CAD FIGURES.....</b>	<b>46</b>
8.1. Final Design (Integrated with full OASYS model).....	46
8.2. I-Beam.....	46
8.3. Lead Screw .....	47
8.4. Dust Cover and Bearing .....	47
8.5. Hinge Mechanism .....	48
8.6. Ball Joint.....	49
8.7. Extended View .....	50
8.8. Stowed View .....	50

## **1. Introduction**

### **1.1. Summary**

This report details the design and analysis of the OASYS Leveling Mechanism. The Outer Space Agriculture System (OASYS) is a project underway by the Canadian Space Agency (CSA) which aims to prototype a small-scale bio-regenerative life-support system (BLSS) for deployment on the lunar surface. The objective of this project was to engineer a lightweight, robust support structure to level the system on uneven lunar terrain. The final design utilizes a four-point stabilizing outrigger system with locking hinges to maximize the stability footprint. Vertical adjustment is achieved via independent trapezoidal lead screws, which are protected from abrasive regolith by a stationary dust cover decoupled via custom insert bearings. Ground irregularities are accommodated by articulating ball-and-socket footpads. To withstand the lunar environment, the system utilizes Aluminum 2219-T87 for structural components, Plasma Electrolytic Oxidation (PEO) coatings to mitigate cold welding, and Tungsten Disulphide ( $WS_2$ ) dry lubricant to eliminate outgassing. Detailed analysis validates that all components meet the required safety factors and operational specifications for lunar deployment.

### **1.2. Client**

The client for this project is the Canadian Space Agency (CSA). The project supports the CSA's OASYS project, which aims to advance knowledge in space-based horticulture and bio-regenerative life-support systems (BLSS).

The OASYS prototype is being developed primarily through a collaborative effort involving student teams across Canada. Group 19 developed this leveling mechanism in consultation with Egor Yaritsa from the CSA's Engineering Development and Capability Demonstration branch, who provided the team with the CSA's requirements for the system, and helped govern the overall scope of the project.

## **2. Purpose**

### **2.1. Scope**

The scope of this project encompasses both the requirements and expectations of the CSA (our client) as outlined in section 2.3, and the expectations and requirements of the MECH 325 course curriculum.

The CSA expects a near-complete design for the OASYS levelling mechanism, including a high-level plan for how to meet mission requirements, justification for each chosen design element, and calculations which show that the design elements meet the required specifications and perform adequately. This led to the careful consideration of materials, selection of standard components (bearings, fasteners, etc), and environmental factors such as cold-welding, outgassing, and lunar regolith.

The scope of this project further encompasses the application of the knowledge that the team gained in the MECH 325 – Machine Design course this semester in selecting adequate components and ensuring that sound decisions were made.

## **2.2. Functions**

The high-level functions of the OASYS levelling system are:

- Ability to level OASYS to account for uneven terrain on the lunar surface.
- Provide a stable base for OASYS, minimizing the risk of tipping over.
- Allow for OASYS to be vertically raised and lowered
- Ease of operation for astronauts in an Extravehicular Activity (EVA) setting

## **2.3. Design Requirements**

Design requirements provided to the team by the CSA are presented below. These include requirements for OASYS and those specific to the levelling system.

Relevant OASYS Requirements:

- [RQMT-0005] - Outgassing: All materials used shall have a Total Mass Loss (TML) of less than 1% and less than 0.1% Collected Volatile Condensable Material (CVCM).
- [RQMT-0006] - Environmental Conditions: The proposed greenhouse concept shall be operable in a vacuum environment of  $2 \times 10^{-12}$  Torr.
- [RQMT-0008] - Lunar Dust Resilience: The lunar greenhouse shall be unaffected by abrasive lunar dust and, where required, protect sensitive areas from lunar dust ingress.
- [RQMT-0009] - Thermal Operating Range: The thermal control system of the greenhouse shall maintain an operable temperature while environmental temperature varies between  $-200^\circ\text{ C}$  to  $+100^\circ\text{ C}$ .
- [RQMT-0017] - Greenhouse Assembly: The greenhouse shall not require any in situ assembly.
- [RQMT-0018] – Structure: The greenhouse structure shall support the mechanical static and dynamic loads encountered during its entire lifetime with a minimum factor of safety of 1.4.
- [RQMT-0020] – Lifespan: The greenhouse shall remain operable for a minimum of 6 weeks (two lunar days and one lunar night).

OASYS Leveling System Requirements:

- [RQMT-LS-0001] - The system shall be capable of leveling the base platform on uneven lunar terrain, compensating for slope or surface irregularities up to  $\pm 15$  degrees from horizontal.
- [RQMT-LS-0002] - The system shall be capable of supporting and leveling a distributed load of up to 130 kg under lunar gravity conditions.

- [RQMT-LS-0003] - The leveling system shall function independently of the system's dedicated electrical power supply and may utilize external power sources, such as auxiliary tools.
- [RQMT-LS-0004] - The system shall not require hydraulic or pneumatic actuation.
- [RQMT-LS-0005] - The leveling accuracy shall be within  $\pm 1^\circ$  of horizontal.
- [RQMT-LS-0006] - The system shall provide adjustable height functionality while maintaining a minimum clearance of 1 meter from the ground to the highest point of the structure when leveled.
- [RQMT-LS-0007] - The system shall fit within an envelope measuring 1020 mm  $\times$  660 mm in its fully stowed configuration.

## 2.4. Evaluation Criteria

The client did not define specific quantitative thresholds for the evaluation criteria. Instead, these factors served as qualitative design drivers to guide decision-making and selection rather than via a numerical scoring matrix.

- System Mass - optimize for low mass, primarily to reduce costs, especially those associated with launching payloads to outer space
- Ease of operability - simplicity and accessibility in deployment and operation considering the experience of the envisioned astronaut operators
- Robustness - aim to minimize systems of failure, including risk of tipping, effects of hard-to-predict factors (cold welding, lunar regolith, etc.)

In addition to these, the team aimed to limit complexity in the design, ensuring that it could be developed within the span of the four-month MECH 325 academic course.

## 2.5. Key Components

The leveling mechanism comprises two categories of components: those involving detailed course analysis relevant to MECH 325, and broader structural components.

1. MECH 325 Relevant Components:
  - a. Lead Screw: TR32x10 trapezoidal screw for vertical adjustment of the system
  - b. Bearings: Insert bearings (deep groove ball bearings) to decouple lead screw and dust cover
  - c. Pins: To lock hinge in place
2. System & Structural Components:
  - a. Deployable Stabilizer Legs: legs swing outward from the chassis to increase the stability footprint
  - b. Hinge and Locking Mechanism: Allows legs to be locked in open and closed positions for deployment and transport
  - c. Dust Cover: A stationary housing to protect the thread shafts from abrasive lunar regolith
  - d. Ball-and-Socket Foot Pads: Articulating pads to adapt to uneven terrain, minimizing bending moments in the screw

### **3. Analysis**

#### **3.1. Assumptions and Simplifications**

Assumptions provided by CSA:

- Dimensions of the main OASYS structure are [850mm (L) x 550mm (W) x 700mm (H)]
- Fixtures can be mounted on any surface of the OASYS structure, excluding the top surface
- The center of mass is located within a volume equal to 20% of the structure's length, width, and height from the geometric center of the OASYS structure in those axes

Assumptions for analysis:

- Consider worst case loading when system is on a 15° slope
- Worst case loading scenario for outrigger beams occurs when entire system load rests on one leg (momentary tipping of system) under terrestrial conditions
- Lunar gravity is taken as  $g_{\text{moon}} = 1.62 \text{ m/s}^2$ , earth gravity is taken as  $g_{\text{earth}} = 9.81 \text{ m/s}^2$

#### **3.2. Inputs**

- System Mass – 130kg (210.6 N with Lunar Gravity)
- Input Torque to raise legs – 1.49 N-m
- NASA Pistol Grip Tool Power – 17 W

#### **3.3. Materials**

##### **3.3.1. Structural – Aluminum 2219-T87**

Aluminum 2219-T87 was selected as the primary structural material due to its heritage in space missions and optimal balance of mass, strength, thermal properties, and machinability. With a density of 2840 kg/m<sup>3</sup> (approx. 1/3 that of steel) and a yield strength of 393 MPa, it provides the optimal strength to weight ratio. Operational risks are mitigated by the alloy's properties. Fatigue failure is ruled out as cyclic stresses aren't present, and creep is negligible as the maximum operating temperature (100°C) remains below 40% of the melting temperature threshold (~220°C). Crucially, the alloy's Face-Centered Cubic (FCC) structure alleviates ductile-to-brittle transitions, ensuring the structure remains ductile at cryogenic temperatures.

##### **3.3.2. Lubricant – Tungsten Disulfide (WS<sub>2</sub>)**

A Tungsten Disulfide dry lubricant was found to be the optimal lubricant solution for various applications in this project, specifically all bearings, and the ball and socket joint for the footpads. Tungsten disulfide has historical usage as dry lubricant for aerospace applications. It can operate at extreme temperatures, has minimal outgassing, and provides low coefficients of friction throughout its allowed operating conditions, making it an ideal candidate for usage in this project.

### **3.3.3. Surface Treatment – Plasma Electrolytic Oxidation (PEO)**

To mitigate the risk of cold welding, the spontaneous fusion of contacting metal surfaces in vacuum, all dynamic aluminum interfaces (hinge assembly and lead screw) are treated with a Plasma Electrolytic Oxidation (PEO) coating. This process converts the surface of the aluminum into a hard, dense, ceramic oxide layer. This ceramic layer eliminates direct metal-on-metal contact, effectively preventing cold welding. The effectiveness of this specific coating on Al 2219 has been validated by the European Space Agency (ESA) in the STM-279 cold welding database. Additionally, PEO provides a characterized coefficient of friction, which was utilized as a validated input for the torque analysis on the threaded shafts.

### **3.3.4. Dust Cover – Fluorinated Ethylene Propylene (FEP)**

Fluorinated Ethylene Propylene (FEP) was selected for the dust protection bellows due to its exceptional thermal stability and vacuum compatibility. It remains flexible at cryogenic temperatures (-240° to 205° C) and satisfies strict NASA outgassing requirements 0.01% TML, 0.0% CVCM). Mechanically, FEP offers a critical balance of flexibility for axial compression and torsional rigidity. Unlike soft fabrics, FEP can resist the internal drag torque from the bearings without twisting or collapsing, ensuring the cover maintains its shape during operation.

## **3.4. Lead Screw**

### **3.4.1. Finalized Lead Screw Specs:**

To allow for vertically raising and lowering the system, it was decided to use four custom designed lead screws. The specifications of the lead screws were chosen according to the following requirements:

- Support the load of the system (130 kg).
- Self-locking to keep the system raised without power input.
- Minimize number of rotations required for deployment.
- Prevent binding to the nut due to misalignment of the lead screw.

A custom lead screw that satisfies these requirements was designed with the threaded portion based off a TR32x10 Metric Trapezoidal Screw. A machined smooth section sits just above the threaded portion, to allow fitting of a ball bearing. Finally, a 70mm hex profile is machined at the top for power input used to raise and lower the system. Two insert bearings, one below the hex head and one at the opposite end of the shaft, are placed to support the bearings that decouple the dust cover from the lead screw. The trapezoidal thread profile was chosen for ease of machineability. Given that this is a custom part, it is beneficial to choose a thread profile that is easier and cheaper to machine. Efficiency is not a significant consideration for this design; hence the trapezoidal thread profile is sufficient. Figure 1 below shows a 3D rendered visual of the custom lead screw.



Figure 1: TR32X10 Lead Screw

The driving factor for the screw diameter was the bending stress due to the weight of the system. The design force for the screw was found to be 163.45N, based on the weight of the system in lunar gravity, and the CSA's specified safety factor of 1.4. For bending analysis, the screw was treated as a solid rod. The minimum rod diameter to withstand bending was treated as the minimum allowable screw root diameter, and a screw was chosen based on this factor. Following this, bearing stress and critical buckling load were calculated and safety factors were found using the yield stress of the aluminum alloy (393 MPa). Further, all the thread stresses and torsions were used to determine the equivalent Von Mises stress and safety factor. Note that calculations assumed the worst-case center of gravity (20% off system's geometric center), and the screw was treated as being 700mm long to allow significant extra extension. Upon further discussion with the CSA, it was decided that a screw length of 400mm would be sufficient. Full analysis is covered in Appendix 7.1.

### 3.4.2. Binding Calculation:

A possible issue identified with the lead screw design is binding of the screw within the nut, due to angular misalignment allowed by the screw/nut thread tolerances. Calculations were done using the ISO 2904:1977 thread tolerances, to determine the nut length required to prevent binding. Elongating the nut minimizes the maximum allowable angle for misalignment. It was determined that the minimum nut length to prevent binding is relatively short. A nut length of 48 mm was selected to allow for enhanced stability and ensure full thread engagement.

Safety factors for the lead screw along with final dimensions are presented in Table 1 and Table 2 below:

Table 1: Lead Screw Loads

	Design Force	Critical Buckling Load	Bearing Stress	Von Mises Stress	Bending Stress
Force/Stress	163.45 N	21.962 kN	-0.388 MPa	2.4 MPa	281 MPa
Safety Factor	1.4	134.4	1012.9	164.6	1.4

Table 2: Lead Screw Specifications

Dimension	D	D <sub>p</sub>	D <sub>r</sub>	p	L	λ	Nut Length
Value	32 mm	26.85 mm	21 mm	10 mm	400 mm	6.761°	48 m

### 3.4.3. Raising & Lowering Forces and Torques:

The torques required to raise and lower the system were calculated using the dynamic friction coefficient of the PEO coating. Based on the lead angle and design force, the raising and lowering torques and forces were calculated. The efficiency was also calculated for completeness, but is not an important criterion, as the screws will only be driven for a very short period. Further, the raising and lowering speeds were calculated, and are further discussed in Section 4.2 - Power Requirements.

Key values summarized in Table 3 below:

*Table 3: Raising and Lowering Loads and Stresses*

	Raising Force	Lowering Force	Raising Torque	Lowering Torque	Efficiency
Value	107.5 N	58.86 N	1.487 Nm	0.825 Nm	17.5 %

### 3.5. Stabilizer Beam and Hinge (Including Pin/Bolt Analysis for Hinge)

The properties, benefits and drawbacks of various beam profiles were compared to help select the most optimal according to the evaluation criteria in Table 4 below.

*Table 4: Comparison of Beam Profiles*

Beam Type	Pros	Cons	Comments
I-Beam	<b>Excellent in vertical bending, efficient for unidirectional loads, good weight efficiency.</b>	<b>More difficult to fabricate than some alternatives.</b>	<b>Aligns well with expected loads and evaluation criteria.</b>
Box Beam	High torsional rigidity, strong biaxial bending, resistant to buckling.	Not as efficient weight wise for uniaxial bending.	Needlessly inefficient since load will be uniaxial.
Circular Tube	Uniform stress distribution, best for torsion loading, and good for biaxial loading.	Difficult to connect to other parts, harder to manufacture.	Inefficient for uniaxial loads, no torsion is expected, and hard to connect to other parts.
Truss Beam	High stiffness to weight, good for very long spans	Many parts make up the truss, usually used for very long spans (not our application)	Multi-part assembly is overly complicated for a short outrigger

The I-Beam cross section was chosen for its superior performance and mass efficiency for uniaxial bending loads, since minimal torsion and other loads will be present (none in ideal steady-state). The I-Beam dimensions seen in Table 5 below were selected in the process of sizing the beam and hinge assembly (calculations presented in Appendix 7.2):

Table 5: I- Beam Dimensions

Flange thickness (mm)	<i>h</i>	6
Web thickness (mm)	<i>b</i>	4
Height (mm)	<i>H</i>	68
Width (mm)	<i>B</i>	63
Area Moment of Inertia ( $\text{mm}^4$ )	<i>I<sub>xx</sub></i>	787322.6667

These dimensions allow for high load bearing with minimal mass, which meets the requirements and performs well according to the design criteria. The I-beam design with the lead screw nut and hinge interface can be seen in Figure 2 below.

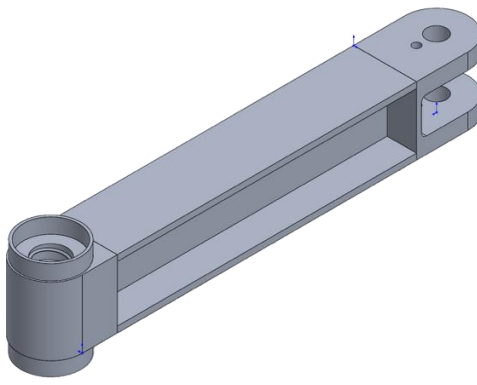


Figure 2: I-Beam Design

### 3.5.1. Beam – Hinge Lock Assembly

The hinge lock assembly is a critical structural component of the stabilizer system, responsible for enabling controlled deployment of the I-beam support leg while safely transmitting bending and torsional loads. The design employs a hinge mechanism, locked via pin, allowing for discrete angular increments, ensuring reliable and repeatable deployment under lunar environmental constraints where regolith, temperature extremes, and limited servicing demand high robustness and simplicity.

The hinge consists of a 20 mm diameter central shaft passing through a 16-36-16 mm stacked plate assembly and secured using an M18 × 1.5 nut. The middle plate incorporates a series of holes spaced at 37° increments allowing for varying locking positions, enabling a total swing of 185° and allowing the outrigger to consistently achieve an optimal deployment angle of 32°. All non-loadbearing interfaces within the hinge are intentionally designed with sufficient clearance to prevent jamming due to lunar regolith incursion, removing the need for additional dust covers or sealing mechanisms. The mechanical load path is carried exclusively through the solid hinge shaft and surrounding plate interfaces, as such, the locking pin engages only in rotation control and does not carry any axial load, ensuring predictable and reliable structural behavior. The calculations for the sizing of this central shaft can be found in Appendix 7.2. Figure 3 below shows the Computer-Aided Design (CAD) model of the mechanism and the fasteners.

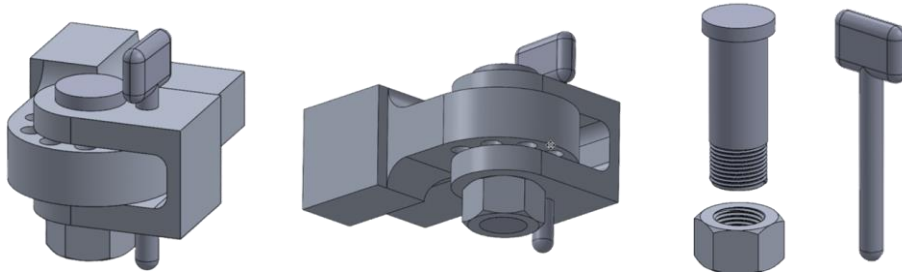


Figure 3: Hinge Lock Mechanism

This hinge design was selected because it provides a combination of a robust single axis rotational interface, discrete and repeatable locking positions that do not degrade under wear, extremely low mechanical complexity, and a direct and traceable load path through a solid shaft rather than through slender linkages or multi-piece mechanisms.

The hinge and I-beam support legs were sized together due to functioning as a single structural system. Due to the hinge being the most geometrically constrained component and carrying the most complex loading, it was expected to control the overall safety factor of the outrigger. To support this design approach, the I-beam was selected as the smallest profile capable of safely carrying the applied bending loads. Using this minimum size beam ensured that its safety factor remained high, while the hinge's safety factor became the closest to the required value of 1.4. This establishes the hinge as the governing component in the design, while the I-beam remains safely above required structural limits. This design method ensures a predictable load path, clear identification of the controlling element, and reliable structural performance.

Extensive FEA analysis was done using SOLIDWORKS Simulation to verify that the hinge assembly satisfies requirements under the maximum predicted loads, and that the stress is transmitted through the assembly as expected. All components were modelled as Aluminum 2219-T87, and details of the FEA analysis can be found in Appendix 7.2.

### 3.6. Dust Cover

#### 3.6.1. Preliminary Design

To protect the lead screw and bearings from abrasive lunar regolith, a flexible dust cover was integrated into the leg assembly. The design employs a bellow geometry to accommodate the full vertical motion of the extending leg while maintaining a sealed enclosure. The bellows are mechanically decoupled from the rotating lead screw via custom insert bearings, ensuring the cover remains stationary during actuation. The lead screw's bolt head and a locking nut clamp firmly onto the bearing's extended inner ring, creating a single rotating assembly. The stationary dust cover is bonded to the bearing's outer ring, allowing the threaded shaft to spin freely inside while the cover remains static and sealed.

A preliminary pleated bellows design was modeled to verify assembly. The geometry incorporates radial clearance between the lead screw threads and the bellows inner wall to effectively eliminate the risk of interference or wear during operation. The design can be seen in Figure 4 below.

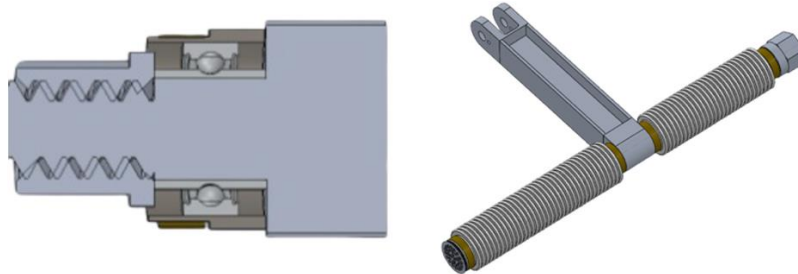


Figure 4: Bearing Location (Left) and Dust Cover Design(Right)

### 3.7. Bearings

The method for selecting bearings prioritized geometric integration, assembly, reliability, and environmental survival over standard load-capacity sizing. To decouple the rotating lead screw from the stationary dust cover housing, a custom unit based on the SKF YAR-206 series geometry was selected. Table 6 below lists the specifications of the bearing

Table 6: Bearing Specifications

Model	SKF-YAR-206-104-2F	Customized
Bore Diameter (mm)	31.75	32
Outside Diameter (mm)	62	62
Width (mm), Inner Ring	38.1	38.1
Width (mm), Outer Ring	18	18
Rolling Element	Balls	Balls
Housing Material	Carbon Chromium Steel	Al 2219-T87
Ball Material	Bearing Steel	$\text{Si}_3\text{N}_4$
Lubricant	Grease	$\text{WS}_2$
Seals	NBR	FEP
Cold-welding treatment	-	PEO

#### 3.7.1. Selection:

Unlike typical applications where bearings are sized to match the load, this selection was driven by the structural requirements of the lead screw. The bore diameter was dictated by the lead screw major diameter of 32mm. While a 32 mm bore bearing possesses a load capacity far exceeding the system's operational requirements, reducing the bearing size would have required stepping down the shaft diameter, which was not practically possible.

The YAR-206 series was selected specifically for its geometry. It is a sealed deep groove ball bearing with an extended inner ring. Standard deep-groove ball bearings typically have flush faces. In this design, a standard bearing would have interfered with the lead screw bolt head or the locking nut, causing undue friction and potential failure. The extended inner ring solves this issue by acting as a built-in spacer, moving the contact surface away from the seals and outer ring, ensuring that the locking nut applies force only to the rotating inner ring. This prevents binding and friction between the rotating lead screw and the stationary dust cover. Figure 5 below shows the geometry of the bearing with the extended inner ring.

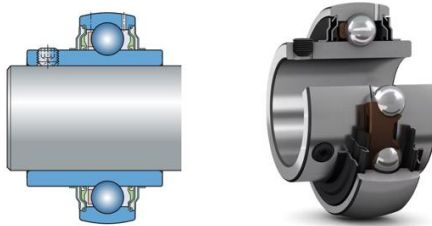


Figure 5: SKF-206-104-2F Bearing

### 3.7.2. Modifications:

Commercial-off-the-shelf (COTS) bearings utilize materials incompatible with the lunar environment. The selected bearing utilizes the SKF bearing's geometry but specifies the following custom modifications:

- Bore Diameter: A 32mm bore diameter will be required as SKF does not produce the Y-series in that size. The closest is 1.25" (31.75 mm), which is selected for preliminary analysis.
- Housing Material: Al 2219-T87 recommended in place of steel. Lighter, better operating temperature range, and thermal expansion not an issue. PEO coating provides required hardness.
- Ball Material:  $\text{Si}_3\text{N}_4$  recommended as it can provide the required hardness while not causing issues due to thermal expansion, or temperature operating range.
- Lubrication: Typical grease lubricant outgasses and solidifies in vacuum/cryogenic conditions. Recommended replacement with  $\text{WS}_2$  dry film lubricant, which maintains a coefficient of friction as low as 0.03 in vacuum.
- Sealing: NBR seals recommended to be replaced with FEP, the same material as the dust covers, to pass the outgassing and temperature requirements.
- Cold Welding Treatment: PEO coating recommended to prevent cold-welding between the bearing housing and shaft, as well as provide a hard layer for the ball bearings.

### 3.7.3. Performance Analysis

Quantifying the performance of the custom bearing was out of the scope for the project, so the SKF bearing's parameters were used to for the purposes of analysis. The calculations can be found in Appendix 7.3. Key findings are presented in Table 7 below. The bearings do not experience much load. Loads experienced are due to weight and spring force of the dust cover. The weight was estimated to be 0.26N using the volume determined from SOLIDWORKS, which is relatively negligible. Determining the spring force was deemed out of scope, so it was estimated to be 50N.

Table 7: Bearing Analysis Results

Parameter	Value	Acceptable Limit
Speed	196.7 RPM	<6300 RPM
Lifetime	1008 Hours (6-weeks)	$<5.021 * 10^9$ Hours
Static Load	50N	<11200 N
Static Safety Factor	448	>1.4

The analysis demonstrates substantial safety margins across all critical performance metrics. These margins are a direct consequence of the sizing strategy, where the bearing dimensions were dictated by the 32 mm shaft diameter rather than the relatively low operational loads. These large safety margins leave space for further analysis with the custom bearings.

### 3.8. Ball Joint

The main design considerations for the ball joint were that it has a range of articulation of 15.2 degrees, withstand the harsh thermal conditions of the lunar surface, and withstand the weight of the system. Full calculations shown in Appendix 7.4.

The design load for the ball joint was the full system weight, representing the worst-case loading scenario. For a payload weight of 30 kg and safety factor of 1.4, the gravitational load is calculated to be  $F_{weight} = 68.04\text{ N}$ .

Due to ball joints being inherently robust, structural integrity was not a major design concern. To maintain dimensional consistency with the rest of the system, the neck of the ball was selected to have an 18 mm diameter, matching the minor diameter of the lead screw. For a given neck diameter, the ball diameter must be over 1.6 times larger, so that there is enough overhang on the lower hemisphere of the ball (which is not occupied by the neck) for the socket to encompass, in order to retain the ball.

$$D_{ball} = 30\text{mm}$$

After the ball dimensions were finalized, the clearance between the ball and socket were calculated. To determine the clearance, the worst-case thermal conditions were assumed. In this case, the socket and ball will encroach towards each other and will seize if the clearance is not properly calculated. Taking a coefficient of thermal expansion of  $\alpha = 23 \cdot 10^{-6}$  for aluminum 2219-T87 and considering a reference room temperature as 20 degrees Celsius: the ball expansion was calculated as 0.055 mm, while the socket contraction would be  $-1.2\text{ mm}$ . Summing them together, the total thermal displacement would be 0.175mm . Therefore, the clearance must be greater than 0.175mm. The clearance must not be too large, or the ball will fit too loosely inside the socket. A clearance,  $C = 0.25\text{ mm}$ , was chosen as an appropriate value.

Knowing the clearance and articulation angle, as well as ball and neck diameters, the socket opening radius was determined to be 23.5 to ensure that the opening diameter of the socket would be large enough to not geometrically interfere with the neck of the ball before the required articulation angle is reached.

One important parameter for assessing the integrity of a ball joint is the retention overlap, which represents how far the socket encompasses the ball. We designed it to be 3.25 mm, a conservative value for ball joints.

Next the failure loads of the ball joint in tensile and compressive modes were determined. The joint will mainly be subjected to compressive loads as it supports the system, but the tensile loads were still calculated for the sake of thoroughness.

For aluminum 2219-T87:  $\sigma_{yield} = 350\text{Mpa}$ ;  $\tau_{yield} = 200\text{MPa}$

The compressive failure load was calculated to be 89 kN, representing the load which would end up crushing the neck, which has the smallest cross sectional surface area. The tensile failure load was determined as 48 kN, the minimum tensile load which would shear the socket walls enough to pull the ball out.

When the ball is at its maximum articulation of 15 degrees, the neck will experience 0.069 MPa of shear stress, which is way smaller than 200 MPa, the shear yield stress of aluminum.

It was concluded that the stresses experienced by the joint under 68 N of force will be well beneath the expected failure stresses. Therefore, the joint design was considered sound and complete.

The ball joint design can be seen in Figure 6 below.



Figure 6: Ball Joint Design

## 4. Results

### 4.1. Final Design

The OASYS leveling mechanism utilizes a four-point independent stabilizer architecture to provide stable leveling on slopes of up to  $\pm 15^\circ$  inclination. The system is presented in Figures 7 & 8 below, and in larger scale in Appendix 8.7 & 8.8. The system integrates four primary mechanical sub-assemblies:

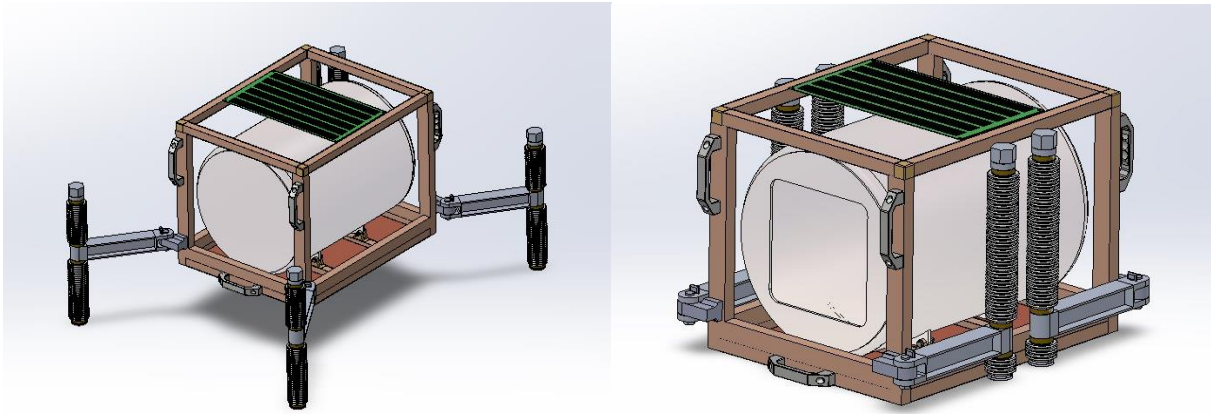
**Structural Outrigger:** Deployable I-beam arms pivot on a locking hinge to increase the system's stability footprint while simultaneously minimizing stowage volume. Once deployed, the arms are secured via pins to resist lateral torque.

**Height Adjustment:** Vertical motion is driven by a TR32x10 trapezoidal lead screw. The 32 mm diameter ensures column stability against the 130 kg load, while the 10 mm pitch allows fast deployment and provides self-locking capability to hold position without power.

**Dust Protection:** A flexible FEP corrugated dust cover is mechanically decoupled from the rotating lead screw via custom insert bearings. This configuration ensures the dust cover

remains stationary and sealed during actuation, protecting the drive components from regolith.

**Ground Interface:** Articulating ball-and-socket footpads provide 23° of angular freedom. This ensures the pads conform to uneven terrain, protecting the lead screw from severe bending moments.



*Figures 7 & 8: The OASYS Levelling Mechanism, shown in deployed and stowed forms*

## 4.2. Power Requirements

To satisfy CSA Requirement RQMT-LS-0003 (Power Independence), the leveling system may be manually actuated via a separate hand crank tool. Torque analysis (7.1) indicates a required input of 1.49 Nm to raise the system.

While the amount of force that an astronaut will be able to exert in lunar conditions is difficult to quantify due to relying on a number of factors such as their personal strength and the EVA suit being worn, it is expected that this value will be more than sufficient to actuate the system. The manual crank tool was designed to accommodate the ergonomics and dexterity limitations associated with being in an EVA suit.

Alternatively, a power tool suitable for lunar conditions can be used to actuate the system. The National Aeronautics and Space Administration (NASA)'s Pistol Grip Tool (PGT), currently in use aboard the International Space Station (ISS) is designed for use in low gravity environments, and is considered to be suitable for this application.

Based on documentation regarding the PGT, the raising and lowering rate of the system when actuating via the PGT were determined. The maximum power output was found to be 17.01 W. This yields a raising (deployment) speed of 18.2 mm/s and a lowering (retraction) speed of 32.8 mm/s. Based on this, the system can be fully deployed in just over a minute and fully retracted in just over thirty seconds (disregarding time spent moving between legs). Note that calculations assume each leg is fully extended by 300 mm, actual timing may vary depending on the inclination of the ground. A summary is shown in Table 8 below, and full calculations can be found in Appendix 7.1.

*Table 8: Leg Deployment Time*

Parameter	Raising Speed	Raising RPM	Raising Time (4 Legs)	Lowering Speed	Lowering RPM	Lowering Time (4 Legs)
Value	18.2 mm/s	109.2 rpm	66 s	32.8 mm/s	196.9 rpm	36.6 s

### **4.3. Safety Factors**

All design components meet the minimum safety factor requirement of 1.4. Safety factors for the various components can be found in Table 9 below

*Table 9: System Safety Factors*

Component	Lead Screw	Ball Bearings	Hinge Assembly	I-beam	Ball and Socket Joint
Safety Factor	1.4	448	2.65	108	705

## **5. Conclusions and Recommendations**

### **5.1. Summary**

The OASYS Leveling Mechanism successfully meets all client requirements for deploying and stabilizing OASYS. The final design utilizes a four-point independent stabilizer system to provide a stable, level platform on uneven terrain with slopes up to  $\pm 15^\circ$ . Detailed mechanical analysis confirms that the system is structurally robust. The TR32x10 lead screw and outrigger beams withstand the 130 kg static load with significant safety margins, effectively mitigating risks of yielding, bending and buckling under worst-case loading conditions. All critical components exceed the client's minimum safety factor requirement of 1.4, with the lowest calculated safety factor being 1.4 for the lead screw. Furthermore, the design explicitly addresses the unique challenges of the lunar environment. The implementation of custom insert deep groove ball bearings, tungsten disulphide dry-film lubrication, and PEO surface treatment effectively mitigate the risks of regolith abrasion and jamming, outgassing, and cold welding.

### **5.2. Future Actions**

**Synchronized Actuation & Stability:** The current manual lifting procedure requires iterative, sequential adjustments to prevent dangerous chassis tilt and payload shifting. Future development may prioritize implementing a synchronized actuation mechanism to enable actuation of all legs simultaneously, reducing structural risk and deployment time.

**Soil-Structure Interaction:** The current analysis assumes a rigid ground interface. Future work may incorporate lunar regolith soil mechanics to verify that footpad pressure does not over-exceed the soil's bearing capacity, preventing excessive沉降 or differential settlement.

**Optimize Mass:** While the design was created with reducing mass in mind, extensive analysis for mass reduction was not performed. The resulting design has large safety factors, indicating room for further optimization.

Dust Cover Analysis: Further analysis may be done to determine the mechanical properties of the dust cover bellows. Spring constant and transmission of torsion need to be further analyzed to ensure failure of bearings or dust covers does not occur.

## **6. References**

### **6.1. Materials:**

<https://asm.matweb.com/search/SpecificMaterial.asp?bassnum=MA2219T87>

<https://www.aac-research.at/services/consulting/coldweld-database/>

<https://brycoat.com/surface-engineering/got-friction-brycoat-dry-film-lubricant-coatings/got-friction-brycoat-tungsten-disulfide-ws2-dry-lubricant-coatings/>

<http://keronite.com/>

[http://esmat.esa.int/Publications/Published\\_papers/Keronite2007paper.pdf](http://esmat.esa.int/Publications/Published_papers/Keronite2007paper.pdf)

<https://etd.gsfc.nasa.gov/capabilities/outgassing-database/>

<https://www.fluorolab.com/wp-content/uploads/2018/02/Teflon-FEP-Film-Information-Bulletin.pdf>

<https://lairdplastics.com/resources/lowdensity-polyethylene-ldpe-complete-technical-guide/>

### **6.2. Lead Screw**

<https://torqbolt.com/iso-2904-metric-trapezoidal-acme-threads-specifications-dimensions>

### **6.3. Dust Cover**

<https://tpsx.arc.nasa.gov/MaterialsDatabase>

### **6.4. Bearings**

<https://www.skf.com/ca/en/products/rolling-bearings/ball-bearings/insert-bearings>

<https://www.skf.com/ca/en/products/rolling-bearings/ball-bearings/insert-bearings/productid-YAR%20206-104-2F>

[https://cdn.skfmediahub.skf.com/api/public/0901d196802809de/pdf\\_preview\\_medium/0901d196802809de\\_pdf\\_preview\\_medium.pdf#cid-121486](https://cdn.skfmediahub.skf.com/api/public/0901d196802809de/pdf_preview_medium/0901d196802809de_pdf_preview_medium.pdf#cid-121486)

[https://cdn.skfmediahub.skf.com/api/public/0901d196802a2b8f/pdf\\_preview\\_medium/0901d196802a2b8f\\_pdf\\_preview\\_medium.pdf#cid-129182](https://cdn.skfmediahub.skf.com/api/public/0901d196802a2b8f/pdf_preview_medium/0901d196802a2b8f_pdf_preview_medium.pdf#cid-129182)

<https://ntrs.nasa.gov/api/citations/20140010477/downloads/20140010477.pdf>

### **6.5. Power Requirements**

<https://ntrs.nasa.gov/api/citations/19960025621/downloads/19960025621.pdf>

## **7. Appendix A – Calculations, Detailed Analysis**

### **7.1. Lead Screw**

See following pages:

Nov 15 2015

$$g = 1.62 \text{ m/s}^2$$

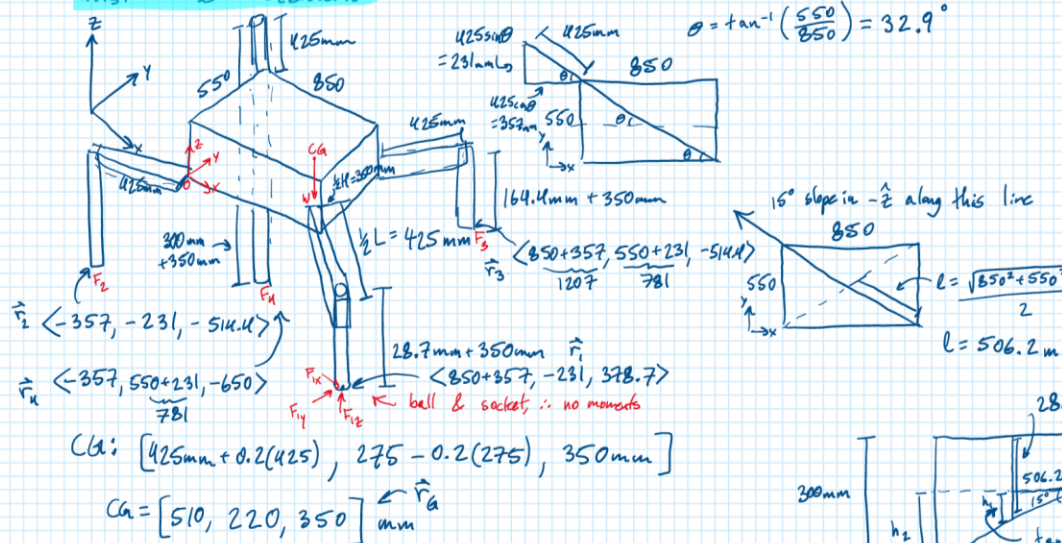
$$W_{\text{days}} = 130 \text{ kg}$$

% Var. (G = 20%)

$$L \times W \times H = 850 \times 550 \times 700 \text{ mm}$$

Max elevation =  $15^{\circ}$

## Worst Case Scenario:



$$\sum F_x: F_{1x} + F_{2x} + F_{3x} + F_{4x} = 0$$

$$\sum F_y: F_{1y} + F_{2y} + F_{3y} + F_{4y} = 0$$

$$\Sigma F_z: F_{1z} + F_{2z} + F_{3z} + F_{4z} = 130(1.62)$$

$$\sum M: \vec{r}_1 \times \vec{F}_1 + \vec{r}_2 \times \vec{F}_2 + \vec{r}_3 \times \vec{F}_3 + \vec{r}_4 \times \vec{F}_4 + \vec{r}_5 \times \vec{W} = 0$$

$$\begin{bmatrix} 1207 \\ -231 \\ 378.7 \end{bmatrix} \times \begin{bmatrix} F_{1x} \\ F_{1y} \\ F_{1z} \end{bmatrix} \rightarrow \begin{bmatrix} -557 \\ -231 \\ -514.4 \end{bmatrix} \times \vec{F}_2 \rightarrow \begin{bmatrix} 1207 \\ 231 \\ -514.4 \end{bmatrix} \times \vec{F}_3$$

The diagram illustrates a stepped foundation with a total height of 300 mm. The top step has a width of 506.2 mm and a depth of 15°. The bottom step has a width of 271.3 mm. The left side shows a vertical height of 300 mm and a horizontal distance of 300 - 271.3 = 28.7 mm. The right side shows the slope angle of 15°. Trigonometric relationships are used to calculate the dimensions of the steps:

$$\tan(15^\circ) = \frac{h_1}{506.2}$$

$$h_1 = 506.2 \tan(15^\circ) = 135.6 \text{ mm}$$

$$\tan(15^\circ) = \frac{h_2}{28.7}$$

$$h_2 = 28.7 \tan(15^\circ) = 271.3 \text{ mm}$$

$$\begin{array}{c} \nearrow \\ \left[ \begin{array}{c} -46.332 \\ 107.406 \\ 0 \end{array} \right] \\ \left. \right\} = 0 \\ 10.6 \end{array}$$

$$\begin{matrix} -231F_{1x} - 378.7F_{1y} & -231F_{2z} + 514.4F_{2y} & +781F_{3z} + 514.4F_{3y} & +781F_{4z} + 650F_{4y} & | \quad 146.332 \\ 378.7F_{1x} - 1207F_{1z} & -514.4F_{2x} + 357F_{2z} - 514.4F_{3x} - 1207F_{3z} & -650F_{4x} + 357F_{4z} & | \quad -107.406 \\ 1207F_{1y} + 231F_{1x} & -357F_{2y} + 231F_{2x} + 1207F_{3y} - 78(F_{3x} - 357F_{4y} - 781F_{4x}) & | \quad 0 \end{matrix}$$

This problem is statically indeterminate

Let's make some assumptions to remove some force

↳ First, we only care about the z forces so let's set x & y forces to zero

By symmetry of the loading we can assume that  $F_{22} = F_{32}$

New system of eq's:

$$\sum F_z: F_{1z} + 2F_{2z} + F_{4z} = 210.6$$

$$EM_x = -0.23(F_{12} - F_{22}) + 0.78(F_{22} + F_{42}) \equiv y_6 - 33$$

$$\sum M_y; -1.207F_{1z} + 0.357F_{2z} - 1.207F_{3z} + 0.357F_{4z} = -1.97 \text{ kip}$$

$$\left[ \begin{array}{ccc|c} F_{12} & F_{22} & F_{42} & \\ \hline 1 & 2 & 1 & 210.6 \\ -0.231 & 0.55 & 0.781 & 46.332 \\ -1.207 & -0.85 & 0.367 & -107.406 \end{array} \right]$$

$$\left[ \begin{array}{ccc|c} 1 & 0 & -1 & 22.89 \\ 0 & 1 & 1 & 93.85 \\ 0 & 0 & 0 & 0 \end{array} \right]$$

$$F_{12} - F_{42} = 22.89$$

$$F_{22} + F_{42} = 93.85$$

↳ I think combining  $F_2$  &  $F_3$  made this unsolvable

↳ I will treat  $F_2$  at 1 force which should make all the forces higher than reality → my resultant design from this will be an overestimation

Solve:

$$\left[ \begin{array}{ccc|c} F_{12} & F_{22} & F_{42} & \\ \hline 1 & | & 1 & 210.6 \\ -0.231 & 0.55 & 0.781 & 46.332 \\ -1.207 & -0.85 & 0.367 & -107.406 \end{array} \right]$$

↳  $F_{12} = 116.75\text{N}$

$$F_{22} = 0$$

$$F_{42} = 93.85\text{N}$$

So the max force one leg should be able to support is  $116.75\text{N}$

$$\frac{116.75\text{N}}{4.448} = \boxed{26.25\text{lbf}}$$

↳ Now, I look at appropriate lead screw sizes to support this weight.

$$\text{Lubricant: } VS_2 - \mu_k = 0.03 - 0.07$$

Metal: Aluminum 2219-T87

- First, I set my design force:

$$F_{des} = F_{nom} \cdot n_{SF} \quad n_{SF} = 1.4 \text{ for CSA}$$

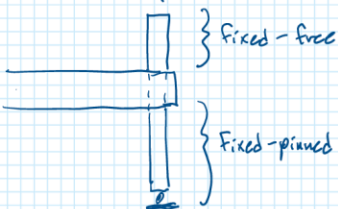
$$F_{des} = 116.75(1.4)$$

$$\boxed{F_{des} = 163.45\text{N}}$$

- Then, solve for critical Euler buckling load

$$P_{cr} = \frac{\pi^2 EI}{(KL)^2}$$

- Effective length is tricky since there are essentially two end fixity scenarios:



- Since we are looking at the leg fully extended, let's only look at the bottom portion (fixed-pinned), and take the nominal length to be  $L_{nom} = 700\text{ mm}$  (max leg length for it to fit within height of OASYS).

$\hookrightarrow K=0.8$  (using practical value, despite theoretical being  $K=0.7$ )  
 $\hookrightarrow L=0.7\text{ m}$

- The Young's Modulus comes from a datasheet for the chosen aluminium  $\rightarrow E=73.1\text{ GPa}$

<https://asm.matweb.com/search/SpecificMaterial.aspx?baseNum=MA2219T87>

- Second moment of area,  $I$ , will use boreal root diameter

$$I = \frac{\pi d^4}{64}$$

$$\Rightarrow P_{cr} = \frac{\pi^2 EI}{(KL)^2} = \frac{\pi^2 E \cdot \frac{\pi d^4}{64}}{(KL)^2}$$

$$d^4 = \frac{64 P_{cr} (KL)^2}{\pi^3 E}$$

$\hookrightarrow$  Want  $P_{cr} \geq F_{des}$

$$d = \left( \frac{64(163.45\text{ N})(0.8 \cdot 0.7)^2}{\pi^3 (73.1 \times 10^9 \text{ Pa})} \right)^{\frac{1}{4}}$$

$$d = 6.17\text{ mm} \quad \underline{\text{which is tiny}}$$

$\hookrightarrow$  This corresponds with an 8 mm metric trapezoidal screw

$\hookrightarrow$  I'll size up to 10 mm and run calculations on whether the threads can support the weight

$\rightarrow$  Choose: ISO Metric trapezoidal power screw

$D=10\text{mm}$ , $p=2\text{mm}$ , $D_p=9.8\text{mm}$ , $D_n(6)=7.5\text{mm}$ , $A_t=53.46\text{mm}^2$
--

- bearing stress from force  $F_{des}$ :

Shigley B-10:  $\sigma_B = -\frac{2F}{\pi D_m^2 p}$   
 $\hookrightarrow$  assume one thread for now

$$\sigma_B = -\frac{2(163.45)}{\pi (9.8 \times 10^{-3})(1)(2 \times 10^{-3})}$$

$$\sigma_B = -5.78 \text{ MPa}$$

- Bending stress at the root of threads:

$$\text{Shigley 8-11: } \sigma_x = \frac{6F}{\pi d r n_b p}$$

$$\sigma_x = \frac{6(163.45)}{\pi(7.5 \times 10^{-3})(1)(2 \times 10^{-3})}$$

$$\sigma_x = 20.81 \text{ MPa}$$

- Compressive axial stress due to force:

$$\text{Shigley 8-8: } \sigma_y = -\frac{4F}{\pi d r^2}$$

$$= -\frac{4(163.45)}{\pi(7.5 \times 10^{-3})^2}$$

$$\sigma_y = -3.7 \text{ MPa}$$

- Find a suitable thread lead angle using:

$$\text{Shigley 8-3: } \mu > \tan \lambda$$

$$\text{Lead angle is given by } \lambda = \tan^{-1} \left( \frac{p}{\pi D_p} \right)$$

$$\tan \lambda = \frac{2 \text{ mm}}{\pi(9 \text{ mm})}$$

$$\tan \lambda = 0.07074$$

For self-locking, we need  $\mu > \tan \lambda$

since  $\mu \approx 0.03 - 0.07$  the screw is on the cusp of self-locking. Let's see if sizing down helps:

$$D = 8 \text{ mm screw, } p = 1.5 \text{ mm, } D_p = 7.25 \text{ mm, } D_r = 6.2 \text{ mm}$$

$$\tan \lambda = \frac{1.5}{\pi(7.25)} = 0.0658$$

$\hookrightarrow$  still on the cusp

$\hookrightarrow$  either a higher friction lubricant is needed or a locking system is necessary. Let's proceed with our original selection assuming this gets sorted out.

- Solve for the various forces for raising/lowering, and the torques

$$\tan \lambda = 0.07074$$

$$\lambda = 4.046^\circ$$

$$P_R = \frac{F(\sin \lambda + \mu \cos \lambda)}{\cos \lambda - \mu \sin \lambda}$$

let  $\mu = 0.07 \rightarrow$  assume highest friction case

$$P_R = \frac{(163.45)(\sin 4.046^\circ + 0.07 \cos 4.046^\circ)}{\cos 4.046^\circ - 0.07 \sin 4.046^\circ}$$

$$\underline{P_R = 132.5 \text{ N}}$$

$$P_L = \frac{F(\mu \cos \lambda - \sin \lambda)}{\cos \lambda + \mu \sin \lambda}$$

$$\underline{P_L = 98 \text{ N}}$$

$$T_R = \frac{FD_p}{2} \left( \frac{\cos\theta \tan\lambda + \mu}{\cos\theta - \mu \tan\lambda} \right)$$

$\theta = 15^\circ$  for trapezoidal threads

$$T_R = \frac{(163.45N)(9 \times 10^{-3} m)}{2} \left( \frac{\cos(15^\circ) \tan(16.046^\circ) + 0.7}{\cos(15^\circ) - 0.7 \tan(16.046^\circ)} \right)$$

$$\underline{T_R = 0.617 \text{ Nm}}$$

$$T_L = \frac{FD_p}{2} \left( \frac{\mu - \cos\theta \tan\lambda}{\cos\theta + \mu \tan\lambda} \right)$$

$$\underline{T_L = 0.458 \text{ Nm}}$$

- Now solve for maximum torsion stress using  $T_R$  (higher torque):

$$\tau_{yz} = \frac{16T}{\pi b_r^3}$$

$$\tau_{yz} = \frac{16(0.617)}{\pi (7.5 \times 10^{-3})^3}$$

$$\underline{\tau_{yz} = 7.44 \text{ MPa}}$$

$$\tau_{zx} = \frac{4T}{\pi b_r^3 n_b p}$$

$$\tau_{zx} = \frac{4(0.617)}{\pi (7.5 \times 10^{-3})^2 (1)(2 \times 10^{-3})}$$

$$\underline{\tau_{zx} = 6.98 \text{ MPa}}$$

- Shigley analysis states that  $\sigma_x, \tau_{xy} = 0$

- Note that experiments show that threads don't share loads equally w/ first thread carrying 0.38F, second carrying 0.25F, etc.

↳ above calculations are therefore an overestimation of the stress state

Screw stress tensor:

$$\vec{\tau} = \begin{bmatrix} 20.81 \text{ MPa} & 0 & 6.98 \text{ MPa} \\ 0 & -3.7 \text{ MPa} & 7.44 \text{ MPa} \\ 6.98 \text{ MPa} & 7.44 \text{ MPa} & 0 \end{bmatrix}$$

- Check for failure using von Mises criterion:

$$\sigma_{VM} = \sqrt{\frac{(\sigma_x - \sigma_y)^2 + (\sigma_x - \sigma_z)^2 + (\sigma_y - \sigma_z)^2 + 6(\tau_{xy}^2 + \tau_{xz}^2 + \tau_{yz}^2)}{2}}$$

$$\sigma_{VM} = \sqrt{\frac{(20.81 + 3.7)^2 + (20.81)^2 + (3.7)^2 + 6(6.98^2 + 7.44^2)}{2}}$$

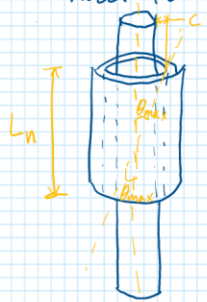
$$\sigma_{VM} = 28.91 \text{ MPa}$$

↳ from material datasheet,  $\sigma_y = 393 \text{ MPa}$  ✓

so screw doesn't fail based on von Mises criterion

- now, let's determine an appropriate nut length to prevent binding
- binding is possible due to the motion of the screw within the nut clearance.

- now, let's determine an appropriate nut length to prevent binding
- binding is possible due to the motion of the screw within the nut clearance.
- ↳ the screw may cock/tilt inside the nut when under load, causing binding
- First, estimate the worst-case tilting due to the screw tolerances
- ↳ model the screw as a shaft in a bearing



Small angle approx:

$$\theta_{\max} \approx \frac{2c}{L_n}$$

Where  $c$  is the radial tolerance of the screw in the nut

- Find an appropriate radial tolerance for 10mm trapezoidal lead screw
- Based on ISO 2904:1977 (most accessible) Metric Trapezoidal Thread tolerances:

#### External Threads (screw):

	$D$	$D_p$	$D_r$
Class 7g, TR 10x2 screw	max 10.00	min 9.820	max 8.929 min 8.739 max 7.5 min 7.191

#### Internal Threads (nut):

	$D$	$D_p$	$D_r$
Class 7H, TR 10x2 nut	min 10.5	min 9.00	max 9.250 min 8.00 max 8.236

<https://torqbolt.com/iso-2904-metric-trapezoidal-acme-threads-specifications-dimensions>

- I believe contact should be measured from the pitch diameters, ∴ the worst-case tolerance would be :

$$\begin{aligned} \theta_{\min, \text{screw}} - \theta_{\max, \text{nut}} \\ = 8.739 - 9.250 \\ = -0.511 \text{ mm } (\underline{\text{loosest fit}}) \end{aligned}$$

- Now, find max tilt angle using

$$\theta_{\max} = \frac{2c_{\text{radial}}}{L_n}$$

$$\theta_{\max} = \frac{0.511}{L_n}$$

→ want to find a suitable  $L_n$  by placing some constraints on  $\theta_{\max}$

- We want  $\theta_{\max}$  to be much less than the lead angle  $\lambda$ , and the friction angle  $\phi = \tan^{-1}(\mu)$  which determines self-locking

$$\lambda = 4.046^\circ$$

$$\begin{aligned} \phi = \tan^{-1}(0.07) &= 4.004^\circ \\ &= \tan^{-1}(0.03) = 1.72^\circ \end{aligned}$$

∴ Want  $\theta_{\max} \ll 1.72^\circ$

For now, set  $\theta_{\max} = 1.72^\circ$  and solve for  $L_n$ :

$$L_n = \frac{2c}{\theta_{\max}}$$

$$L_n = \frac{0.511}{1.72}$$

the required friction to allow self-locking, and check that the raising/lowering torque isn't unreasonable  
 ↳ also see what this friction coefficient is compared to Al on Al contact

November 23, 2025:

### Screw Bending Calculation:

- I'll start by calculating the bending moment due to the force I calculated above

$$\vec{r}_{CA} = [510, 220, 350] \text{ mm}$$

$$\vec{F}_{CA} = [-351, 781, -650] \text{ Nmm}$$

- I'll take the bending moment as the weight  $\times$  the xy distance for the worst-case CA, which is when CA is furthest away from the leg (in the diagram above, leg 4 meets that requirement)

$$F_G = (130 \text{ g}) (1.62 \text{ msc}) (1.4)^{\text{ysef}} = 294.84 \text{ N}$$

$$\vec{r}_{CA} - \vec{r}_{F4} = [867, -561, 1000] \text{ mm}$$

$$d_{xy} = \sqrt{(867)^2 + (-561)^2} = 1027.64 \text{ mm}$$

$$M = (294.84)(1.02764) = \underline{303. \text{ N}\cdot\text{m}}$$

Bending Stress:

$$\frac{\sigma_z}{\gamma} = \frac{M_x}{I_x}$$



- We will idealize the screw, by treating it as a rod of diameter  $D_r$  (root diameter)  
 ↳ Note: this does not consider stress concentration at the threads

- I will look at the max tension point, where  $y = \frac{D_r}{2}$  (-ve, sign just distinguishes compression vs. tension)

$$I_x = \frac{\pi D_r^4}{64} \quad \text{for circ. cross sec}$$

$$\sigma_{z,\max} = \frac{M_x \frac{D_r}{2}}{\frac{\pi D_r^4}{64}}$$

$$\sigma_{z,\max} = \frac{32 M_x}{\pi D_r^3} \quad , D_r = 7.191 \text{ mm} \quad \text{from ISO:1977}$$

$$\sigma_{z,\max} = \frac{32(303)}{\pi (7.191 \times 10^{-3})^3}$$

$$\sigma_{z,\max} = 8.3 \text{ GPa} \gg 393 \text{ MPa}$$

\* This is... fail. I... don't... know.

$$V_{z,\max} = 8.3 \text{ GPa} \Rightarrow 393 \text{ MPa}$$

∴ This design fails due to bending stress

Let's find min. req'd  $D_r$  for bending:

$$\sigma_z = 393 \text{ MPa}$$

$$\sigma_z = \frac{32 M_x}{\pi D_r^3}$$

$$D_r = \left( \frac{32 M_x}{\pi \sigma_z} \right)^{1/3}$$

$$D_r = \left( \frac{32(303)}{\pi(393 \times 10^6)} \right)^{1/3}$$

$$D_r = 1.988 \times 10^{-2} \text{ m}$$

$$D_r = 19.88 \text{ mm}$$

I will pick a TR32x10, whose  $D_{\min}$  is 20.350 mm

So I sized up so much to reduce the number of revs needed to extend 300mm from 150 to 30.

Design choice:

TR32x10 Metric Trapezoidal Screw

$$D = 32 \text{ mm}, D_p = 26.850 \text{ mm}, D_r = 21 \text{ mm}, p = 10 \text{ mm}$$

Let's check  $L_n$  to prevent binding:

ISO 2904:1977

	$D_p$	
Screw	MAX	MIN
TC	26.85	26.45

	max	min
nut	21	20.35

$$\text{Worst fit: } D_{\min \text{ screw}} - D_{\max \text{ nut}}$$

$$26.45 - 21 = 5.45 \text{ mm}$$

$$\lambda = \tan^{-1} \left( \frac{p}{\pi D_p} \right)$$

$$\lambda = \tan^{-1} \left( \frac{10}{\pi(26.85)} \right)$$

$$\lambda = 6.76^\circ$$

$$\phi_{\min} = 1.72^\circ \text{ (From before)}$$

$$L_n = \frac{2c}{\phi_{\max}}$$

$$L_n = \frac{5.45 \text{ mm}}{1.72} = 3.17 \text{ mm}$$

∴  $L_n = 30 \text{ mm}$  is fine

Let's size up to  $1.5 \times D$  for good thread engagement

Let's set  $L_n = 1.5(32)$

$$L_n = 48 \text{ mm}$$

Now let's determine friction needed for self-locking.

$$\mu > \tan \chi$$

$$\boxed{\mu > 0.119} \text{ for self-locking}$$

Which is very reasonable.

November 30, 2025: Final Design:

- Let's verify the stresses & raising and lowering forces

Design Choice:

TR32x10 Metric Trapezoidal Screw

$$D = 32 \text{ mm}, D_p = 26.85 \text{ mm}, D_r = 21 \text{ mm}, p = 10 \text{ mm}$$

$$F_{dS} = 163.45 \text{ N}$$

$$\text{AL 2219-T87} - \sigma_y = 393 \text{ MPa}, E = 73.1 \text{ GPa}$$

Buckling Load:

$$P_{cr} = \frac{\pi^2 EI}{(kL)^2} \quad I = \frac{\pi D_r^4}{64}$$

Values repeated from above, but w/ different  $D_r$ .

$$P_{cr} = \frac{\pi^2 (73.1 \text{ GPa}) \left( \frac{\pi (21 \text{ mm})^4}{64} \right)}{\left[ (0.8)(700 \text{ mm}) \right]^2}$$

$$P_{cr} = 21.962 \text{ kN} \ll F_{dS} \checkmark \\ (163.45 \text{ N})$$

Bearing Stress?

$$\text{Shigley 8-10: } \sigma_B = \frac{-2F}{\pi D_p n_e p} \text{ assume one thread}$$

$$\sigma_B = \frac{-2(163.45 \text{ N})}{\pi (26.85 \text{ mm})(1)(10 \text{ mm})}$$

$$\sigma_B = -0.388 \text{ MPa} \ll \sigma_y \checkmark \\ (393 \text{ MPa})$$

Stresses:

$$\text{Shigley 8-11: } \sigma_x = \frac{6F}{\pi D_p n_e p}$$

$$\sigma_x = \frac{6(163.45)}{\pi (21 \text{ mm})(1)(10 \text{ mm})}$$

$$\sigma_x = 1.49 \text{ MPa}$$

$$\text{Shigley 8-8: } \sigma_y = \frac{-4F}{\pi D_r^2}$$

$$= \frac{-4(163.45)}{\pi (21 \text{ mm})^2}$$

$$\sigma_y = -0.472 \text{ MPa}$$

Raising/Lowering Forces & Torques:

## Raising/Lowering Forces & Torques:

- Using a friction coeff. of  $\mu = 0.6$  based on unlubricated contact of keramite coated surfaces

<https://www.ccg.msm.cam.ac.uk/research-areas/the-plasma-electrolytic-oxidation-peo-process>

Lead angle:

$$\tan \lambda = \frac{F}{\pi D_p}$$

$$\lambda = \tan^{-1} \left( \frac{10\text{mm}}{\pi (26.85\text{mm})} \right)$$

$$\lambda = 6.761^\circ$$

Raising Force:

$$P_R = \frac{F(\sin \lambda + \mu \cos \lambda)}{\cos \lambda - \mu \sin \lambda}$$

$$P_R = \frac{163.45(\sin(6.761^\circ) + 0.5 \cos(6.761^\circ))}{\cos(6.761^\circ) - 0.5 \sin(6.761^\circ)}$$

$$P_R = 107.5 \text{ N}$$

Lowering Force:

$$P_L = \frac{F(\mu \cos \lambda - \sin \lambda)}{\cos \lambda + \mu \sin \lambda}$$

$$P_L = \frac{163.45(0.5 \cos(6.761^\circ) - \sin(6.761^\circ))}{\cos(6.761^\circ) + 0.5 \sin(6.761^\circ)}$$

$$P_L = 58.86 \text{ N}$$

Raising Torque:

$$T_R = \frac{FD_p}{2} \left( \frac{\cos \theta \tan \lambda + \mu \epsilon}{\cos \theta - \mu \tan \lambda} \right)$$

$\theta = 15^\circ$  for trapezoidal threads

$$T_R = \frac{(163.45\text{N})(26.85\text{mm})}{2} \left( \frac{\cos(15^\circ) \tan(6.761^\circ) + 0.5}{\cos(15^\circ) - 0.5 \tan(6.761^\circ)} \right)$$

$$T_R = 1.487 \text{ N}\cdot\text{m}$$

} → This is what the power drill must provide to raise OASYS



IKEA Family price  
TRIXIG  
Screwdriver, lithium-ion, 2.6V

**\$17.99**

20% off, save \$4.40

Regular price: \$21.99  
Price valid Nov 20, 2022 – Nov 20, 2022 or while supplies last.

★★★★★ (10)

Buy today, pay over time with Afterpay. Learn more

② TRIXIG cable and TRIXIG charger are sold separately. Bits are sold separately. Peel-free to complete with TRIXIG bit and disk set.

Complete with

IKEA Family price  
SITTIBJÖRN  
USB-C to USB-C, 1.0 m (3' 3")  
20% off, save \$1.00  
Regular price: \$4.99

Lowering Torque:

$$T_L = \frac{FD_p}{2} \left( \frac{\mu - \cos \theta \tan \lambda}{\cos \theta + \mu \tan \lambda} \right)$$

$$T_L = \frac{(163.45\text{N})(26.85\text{mm})}{2} \left( \frac{0.5 - \cos(15^\circ) \tan(6.761^\circ)}{\cos(15^\circ) + 0.5 \tan(6.761^\circ)} \right)$$

$$T_L = 0.825 \text{ N}\cdot\text{m}$$



This is what 5 N·m of torque looks like :)

Torsion Stresses:

$$\tau_{yz} = \frac{16 T_R}{\pi D_p^3}$$

$$\tau_{yz} = \frac{16(1.487 \text{ N}\cdot\text{m})}{\pi (2\text{mm})^3}$$

$$\tau_{yz} = 0.818 \text{ MPa}$$

$$\tau_{zx} = \frac{4 T_R}{\pi D_p^2 n_p p}$$

$$\tau_{zx} = \frac{4(1.487 \text{ N}\cdot\text{m})}{\pi (2\text{mm})^2 (1)(10\text{mm})}$$

$$\sigma_{zx} = 0.429 \text{ MPa}$$

$$\sigma_z, \tau_{xy} = 0 \text{ by Shigley}$$

Stress Tensor:

$$\bar{\sigma} = \begin{bmatrix} 1.49 \text{ MPa} & 0 & 0.429 \text{ MPa} \\ 0 & -0.472 \text{ MPa} & 0.818 \text{ MPa} \\ 0.429 \text{ MPa} & 0.818 \text{ MPa} & 0 \end{bmatrix}$$

Von Mises Failure Criteria:

$$\sigma_{VM} = \sqrt{\frac{(\sigma_x - \sigma_y)^2 + (\sigma_x - \sigma_z)^2 + (\sigma_y - \sigma_z)^2 + 6(\tau_{xy}^2 + \tau_{xz}^2 + \tau_{yz}^2)}{2}}$$

$$= \sqrt{\frac{(1.49 + 0.472)^2 + (1.49)^2 + (0.472)^2 + 6(0.429^2 + 0.818^2)}{2}}$$

$$\sigma_{VM} = 2.387 \text{ MPa} \ll \sigma_y = 39.3 \text{ MPa} \quad \checkmark$$

December 3, 2025:

- Let's compute the max raising & lowering speeds of the screw using an HST PGAT (Hubble Space Telescope Pistol Grip Tool)
- The reported torque range is 2.7 - 33.9 N·m
- The reported speed range is 0.5 - 6.3 rad/s

<https://ntrs.nasa.gov/api/citations/19960025621/downloads/19960025621.pdf>

Assuming the highest speed corresponds to the lowest torque, I can calculate power output

Power Output:

$$P = T_w$$

$$P = (2.7)(6.3) \quad P = (33.9)(0.5)$$

$$P = 17.01 \text{ W} \quad P = 16.95 \text{ W}$$

Use max power output.

Raising Speed:

$$T_R = 1.487 \text{ Nm}$$

$$n_{raise} = \left( \frac{P_{max}}{T_R} \right) \cdot \left( \frac{1 \text{ rev}}{2\pi \text{ rad}} \right) \cdot \left( \frac{60 \text{ s}}{1 \text{ min}} \right)$$

$$n_{raise} = \left( \frac{17.01}{1.487} \right) \left( \frac{60}{2\pi} \right)$$

$$n_{raise} = 109.2 \text{ rpm}$$

$$V_{raise} = n \cdot p \cdot \frac{1}{60} \cdot \frac{\text{rad}}{\text{min}} \cdot \frac{\text{mm}}{\text{rad}}$$

$$V_{raise} = (109.2)(10) \left( \frac{1}{60} \right)$$

$$V_{raise} = 18.2 \text{ mm/s}$$

↳ If full leg deployment is 300 mm, each leg takes a mm/s

↳ If full leg deployment is 300 mm,  
each leg takes approx:

$$\frac{300 \text{ mm}}{18.2 \text{ mm/s}} = 16.5 \text{ s} \quad \boxed{\text{to deploy}}$$

↳ In the worst case where all 4 legs must fully deploy, deploy time is:

$$4 \times 16.5 \text{ s} = \boxed{66 \text{ s}}$$

(not accounting for time spent moving between legs and levelling).

### Lowering Speed:

$$T_L = 0.825 \text{ Nm}$$

$$n_{lower} = \frac{P_{max}}{T_L} \cdot \frac{60}{2\pi}$$

$$n_{lower} = \left( \frac{17.01}{0.825} \right) \left( \frac{60}{2\pi} \right)$$

$$n_{lower} = 196.9 \text{ rpm}$$

$$V_{lower} = \frac{n \cdot p}{60}$$

$$V_{lower} = \frac{(196.9)(10)}{60}$$

$$V_{lower} = 32.8 \text{ mm/s}$$

One leg lowering time:

$$t_{lower} = \frac{300 \text{ mm}}{32.8 \text{ mm/s}} = \boxed{9.15 \text{ s}}$$

$$4 \times t_{lower} = \boxed{36.6 \text{ s}} \quad \text{to lower 4 legs}$$

### Efficiency:

- For completion, I'll compute the efficiency of our lead screw (though efficiency is not a big concern for our application)

Shigley 8-4:

$$\epsilon = \frac{F_{app} \cdot \text{force to raise}}{2\pi T_R}$$

$$\epsilon = \frac{(163.45 \text{ N})(10 \times 10^{-3} \text{ m})}{2\pi (1.487 \text{ N} \cdot \text{m})}$$

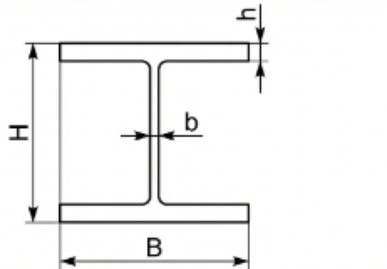
$$\epsilon = 0.175$$

↳ not great, but this is to be expected given our high friction ( $\mu=0.5$ ).

Damye

## 7.2. Outrigger Beam and Hinge (Including Pin/Bolt Analysis for Hinge)

### 7.2.1. Finalized Beam Profile:



Parameter	Variable	Dimension
Flange Thickness (mm)	h	6
Web Thickness (mm)	b	4
Height (mm)	H	68
Width (mm)	B	63

### 7.2.2. Outrigger Beam Bending Analysis: Worst-Case Scenario Justification

Assumptions:

- System mass:  $m = 130 \text{ kg}$
- Lunar Gravity:  $g_{\text{moon}} = 1.62 \text{ m/s}^2$
- Earth Gravity:  $g_{\text{earth}} = 9.81 \text{ m/s}^2$
- Cantilever length from hinge to leg contact point:  $L = 400 \text{ mm}$
- Material yield strength (Al-2219-T87):  $\sigma_{\text{yield}} = 395 \text{ MPa}$
- Required minimum safety factor:  $SF_{\min} = 1.4$

Worst case loading condition: Maximum stress occurs in the case where the system tips so that all load is on one leg, and when the system is under Earth gravity (as opposed to lunar).

**Earth Load:**

$$P_{\text{earth}} = m * g_{\text{earth}} = 1275.3 \text{ N}$$

**Earth bending moment:**

$$M_{\text{earth}} = P_{\text{earth}} * L = 542003 \text{ N * mm}$$

Required Section Modulus:

Allowable stress with safety factor:

$$\sigma_{allow} = \frac{\sigma_{yield}}{SF} = 339.29 \text{ MPa}$$

Required section modulus:

$$S_{req} = \frac{M_{earth}}{\sigma_{allow}} = 1597.48 \text{ mm}^3$$

### **7.2.3. Selected I-Beam Dimensions (see image at beginning of section):**

Flange width:  $B = 63 \text{ mm}$

Overall depth:  $H = 68 \text{ mm}$

Flange thickness:  $h = 6 \text{ mm}$

Web thickness:  $b = 4 \text{ mm}$

### **Computed strong-axis properties:**

$$I_x = 787322.6667 \text{ mm}^4$$

$$S_x = \frac{I_x}{(h/2)} = 23156.54902 \text{ mm}^3$$

This satisfies:  $S_x \geq S_{req}$ .

### **Maximum Bending Stress**

Using:

$$\sigma = \frac{M_{max} * y}{I}$$

$$\sigma_{max} = \frac{M_{max} * (h/2)}{I_x} = 1.82 \text{ MPa}$$

Safety factor:

$$SF = \frac{\sigma_{yield}}{\sigma_{max}} = 217.16$$

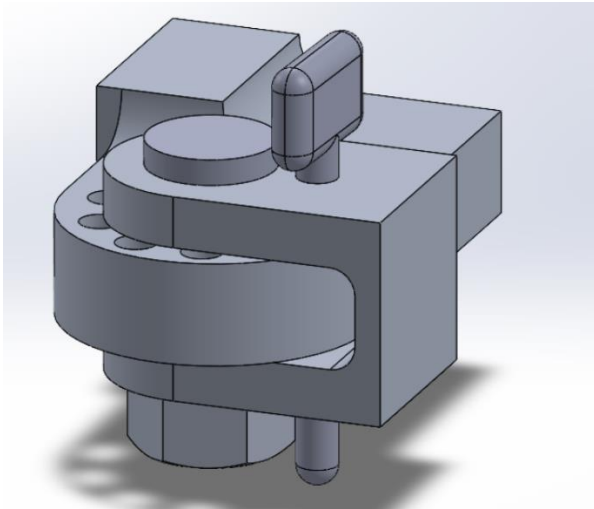
(Well over the required safety factor of 1.4)

### **Conclusion of beam stress calculation:**

The maximum stress on the outrigger occurs only when the system tips onto a single leg. Under this worst-case condition, the load cannot exceed the system weight. The selected I-

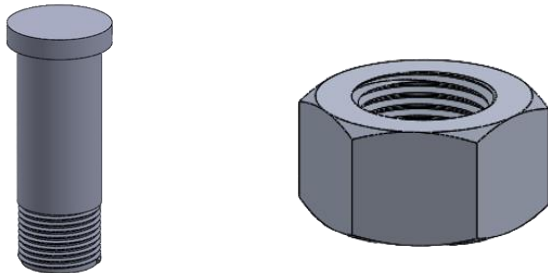
beam profile satisfies the required section modulus and meets the safety factor of 1.4 under Earth load (worst case load).

#### 7.2.4. Hinge, Locking Pin



The above image is of a CAD model of the hinge which connects the outrigger legs to the main body of OASYS. Included in this is a locking pin which allows the hinge to be “locked” into certain angles. Intended operation is as follows: the pin is removed, the outrigger is deployed to the required angle, and the pin is replaced, locking the outrigger at an angle. The pin slides into place to lock the hinge, and a threaded shaft serves as the main hinge component. See Appendix B for more CAD images of this part.

#### 7.2.5. Bolted Connection Analysis for Hinge Joint



The bolted joint consists of a single 20 mm diameter pin passing through a 16-36-16 mm top/middle/bottom plate stack. The joint carries a vertical reaction force from the leg and a twisting moment about the pin axis. The connection is assumed to remain clamped with almost no joint separation. Therefore, no external axial load is transferred into the bolt, and the pin is checked for shear, torsion and bearing.

Parameters:

- 1 Shaft

- Shaft diameter:  $d = 20 \text{ mm}$
- Top plate thickness:  $t_{top} = 16 \text{ mm}$
- Middle plate thickness:  $t_{middle} = 36 \text{ mm}$
- Bottom plate thickness:  $t_{bottom} = 16 \text{ mm}$
- Lever arm:  $r = 400 \text{ mm}$
- Maximum applied torque from the leg:  $T = 75.816 \text{ N} * \text{m}$
- Material: Aluminum 2219-T87
- Target factor of safety:  $SF = 1.4$

Vertical Reaction Force:

The leg-generated torque produces a vertical reaction force at the joint:

$$F_v = T/r = 189.54 \text{ N}$$

### **Shear Stress in the Pin (Double Shear)**

The bolt is in double shear, each shear plane carries half the load.

$$V_{per\ plane} = F_v / 2 = 94.77 \text{ N}$$

Bolt area:

$$Area = (\pi * d^2)/4 = 314 \text{ mm}^2$$

Shear stress:

$$\tau_{shear} = V_{per\ plane}/Area = 0.3018 \text{ MPa}$$

### **Torsional Shear in the Pin**

Conservatively assuming the full applied torque is reacted as torsion in the pin:

$$\tau_{torsion} = (16T)/(\pi d^3) = 48.27 \text{ MPa}$$

$$\tau_{torsion} >> \tau_{shear}$$

Since  $\tau_{torsion} >> \tau_{shear}$ , the combined shear stress is essentially:

$$\tau_{eq} \approx 48.3 \text{ MPa}$$

Allowable shear for 2219-T87 at FOS = 1.4:

$$\tau_{allow} = \text{Shear Strength} / SF = 280 \text{ MPa} / 1.4 = 200 \text{ MPa}$$

Safety factor in shear:

$$SF_{shear} = \tau_{allow} / \tau_{eq} = 4.14$$

The pin passes the shear requirement with a large margin.

## Bearing Stress in Plates

Bearing stress:

$$P = F_v / (d * t)$$

Top plate:

$$P_{top} = F_v / (d * t_{top}) = 0.592 \text{ MPa}$$

Middle block:

$$P_{mid} = F_v / (d * t_{middle}) = 0.263 \text{ MPa}$$

Bottom plate:

$$P_{bottom} = F_v / (d * t_{bottom}) = 0.592 \text{ MPa}$$

Bearing capacity for 2219-T87 exceeds 600 MPa, giving safety factors above 1000. Bearing is not governing.

## Conclusion

The single 20 mm 2219-T87 pin and surrounding plate geometry safely support the applied loading. Combined torsional + direct shear stress in the pin is ~60 MPa, far below the allowable ~200 MPa at FOS 1.4. Bearing stresses in all plates are <0.6 MPa and negligible relative to material capacity. Therefore, the bolted connection is more than sufficient with large safety margins, and no critical axial loading is transmitted to the pin.

### 7.2.6. Bolted Connection Analysis for Locking Pin



The locking pin connection forms the rotational restraint mechanism within the hinge assembly and is responsible for preventing unintended rotation when the outrigger is folded and deployed. While the central hinge shaft carries the primary bending and torsional loads, the locking pin provides rotational restraint by engaging with the pre-set hole patterns in the middle plate. When the pin is inserted, it mechanically blocks rotation and ensures that the hinge remains fixed at the selected deployment angle under operational loading. The locking pin is not part of the axial load path and is instead subjected only to in-plane shear and local bearing where it contacts the edge of the locking hole.

Parameters:

- 1 pin
- Shaft diameter:  $d = 8 \text{ mm}$
- Top plate thickness:  $t_{top} = 16 \text{ mm}$
- Middle plate thickness:  $t_{middle} = 36 \text{ mm}$
- Bottom plate thickness:  $t_{bottom} = 16 \text{ mm}$
- Lever arm:  $r = 20 \text{ mm}$
- Maximum applied torque from the leg:  $T = 75.816 \text{ N} * \text{m}$
- Material: Aluminum 2219-T87
- Target factor of safety:  $SF = 1.4$

The maximum torsional load that the pin may be required to resist is taken from the same worst-case torque applied at the hinge. The locking hole is located at a radial distance  $r$  from the hinge axis, so the torque acting on the hinge plate is converted into a shear force at the pin by:

$$V = T/r = 3790.8 \text{ N}$$

### **Shear Stress in the Locking Pin**

The locking pin behaves as a single-shear member where the hinge plate reaction is transferred across the pin cross-section at the interface with the locking hole. The average shear stress in the pin is calculated as:

Pin area:

$$\text{Area} = (\pi * d^2)/4 = 50.265 \text{ mm}^2$$

Shear stress:

$$\tau_{shear} = \frac{V}{\text{Area}} = 75.41 \text{ MPa}$$

Allowable shear for 2219-T87 at FOS = 1.4:

$$\tau_{allow} = \text{Shear Strength} / SF = 280 \text{ MPa} / 1.4 = 200 \text{ MPa}$$

Safety factor in shear:

$$SF_{shear} = \tau_{allow} / \tau_{shear} = 2.65$$

The pin passes the shear requirement with a large margin.

### **Bearing Stress in the Locking Hole**

Bearing stress:

$$P = V / (d * t)$$

Middle block:

$$P_{mid} = V / (d * t_{middle}) = 13.16 \text{ MPa}$$

Bearing capacity for 2219-T87 exceeds 600 MPa, giving safety factors above 45. Bearing is not governing.

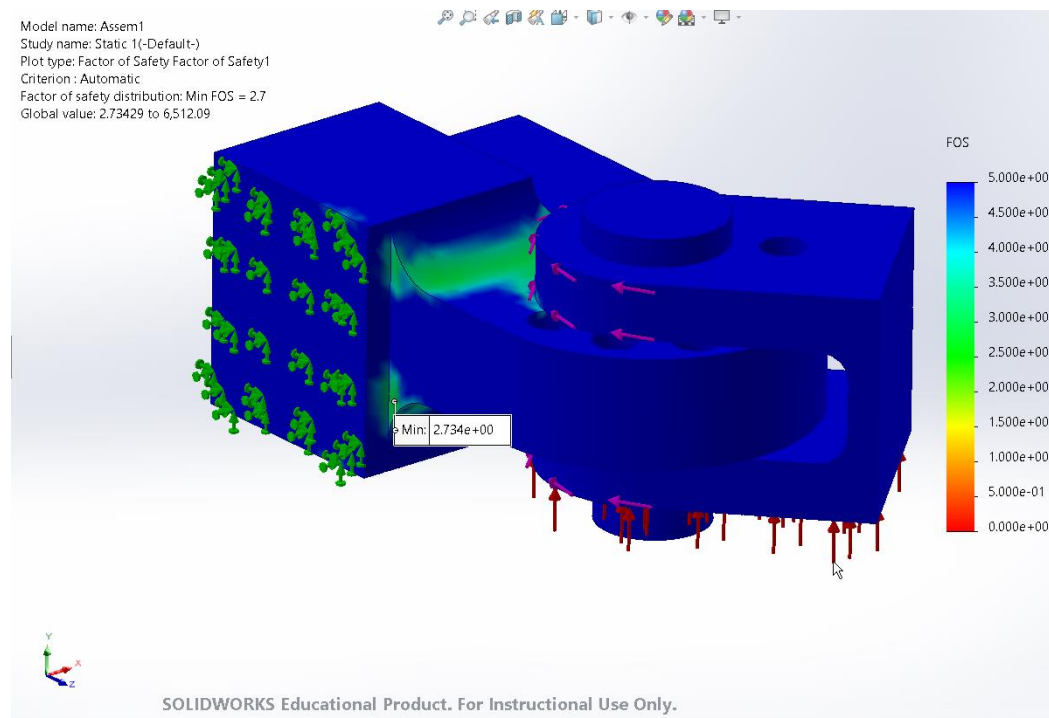
## Conclusion

The locking pin connection is structurally adequate and well matched to the hinge design. It experiences shear-only loading with no axial force and calculations in shear and bearing confirm that it exceeds the minimum required safety factor of 1.4 under the same worst-case loading conditions applied to the hinge shaft.

### 7.2.7. FEA Hinge Analysis/Verification

A comprehensive finite element analysis was conducted in SOLIDWORKS Simulation to verify that the hinge assembly satisfies structural requirements under maximum predicted bending and torsional loads. All components were modeled using Aluminum 2219-T87. Boundary conditions were applied to represent the hinge's fixed interface with the chassis, and external loads were derived from analytical calculations of the maximum torque imposed by the deployed I-beam.

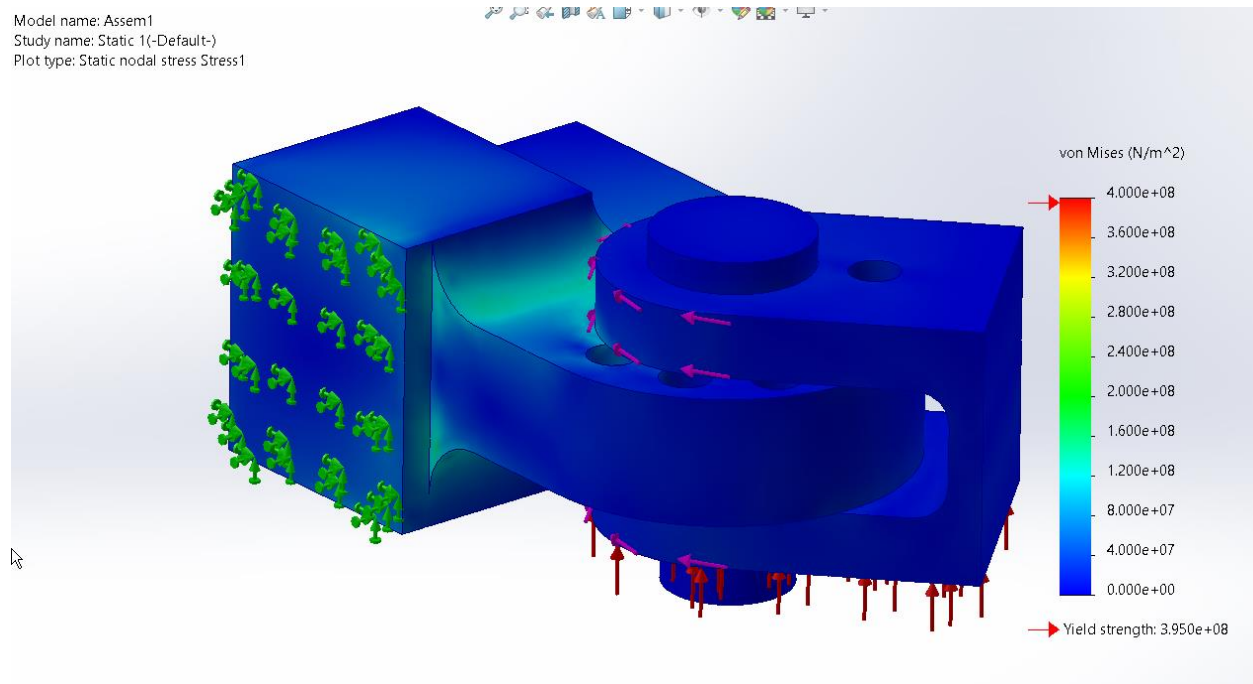
#### Factor of Safety Plot



## Factor of Safety Results

The simulation reported a minimum factor of safety of 2.73, located at the fillet transition between the hinge plate and shaft interface. The remainder of the hinge assembly exhibited safety factors within the 4-5+ range, demonstrating substantial structural margin beyond the required minimum of 1.4.

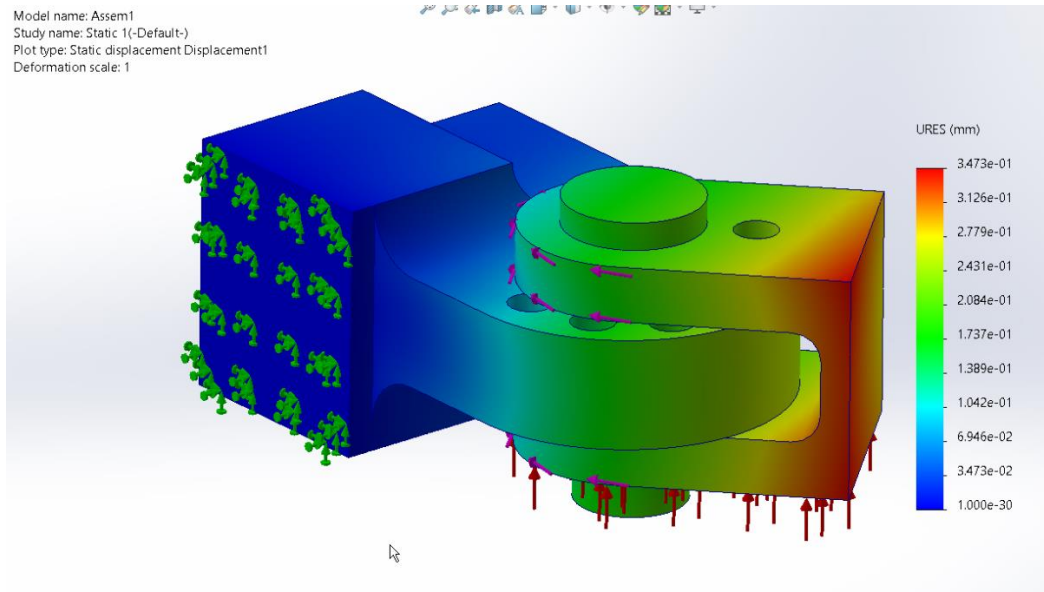
## Stress Plot



## Von Mises Stress Results

The maximum von Mises stress observed in the hinge was 6.26 MPa, representing only 1.6% of the yield strength of Aluminum 2219-T87. This is far below the allowable limit of 279 MPa (yield divided by the required safety factor). Stress concentrations were small, localized, and entirely within the elastic regime.

## Displacement Plot



## Displacement Results

Maximum displacement occurred in the hinge's rotational plate region and was measured at 0.34 mm. This displacement is well within acceptable limits to maintain proper locking hole alignment, engagement reliability, and deployment accuracy. Deformation patterns confirm that the structural load path behaves exactly as designed, passing through the central shaft rather than through the locking pin.

## Conclusion

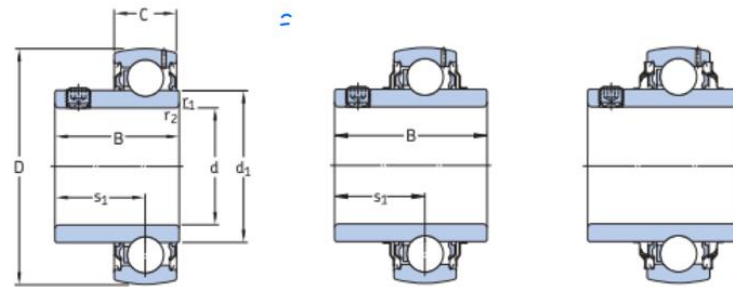
The hinge lock assembly satisfies all structural, functional, and environmental requirements for the outrigger system and demonstrates substantial safety margin in both analytical and numerical evaluations. The combination of a solid shaft load path, discrete pin locking mechanism, and dust tolerant clearances makes this hinge exceptionally well suited for lunar operations where reliability is paramount. FEA and hand calculations consistently verify that the hinge exceeds the minimum required safety factor of 1.4 with significant margin, exhibits minimal stress and deformation under worst case loading, and provides a predictable, stable interface for the deployment of the I-beam support leg. Through careful design with the minimum sized I-beam, the hinge remains the governing structural component, ensuring a high level of confidence in the mechanical performance and readiness of the outrigger system.

## 7.3. Bearings

### SKF Insert Bearing Catalogue Page

Y-bearings with grub screws, inch shafts  
d  $\frac{1}{2}$  –  $\frac{7}{16}$  in

P.95



Dimensions	YAT						YAR-2F			YAR-2RF			Designation	
	d	D	B	C	d <sub>1</sub>	s <sub>1</sub>	r <sub>1,2</sub> min	Basic load ratings		Fatigue load limit P <sub>u</sub>	Limiting speed with shaft tolerance h6	Mass		
								dynamic C	static C <sub>0</sub>					
in/mm								lbf/kN	lbf/kN	r/min	lb/kg	–		
<b>1 <math>\frac{1}{8}</math></b> 28,575	2,4409 62	1.50 38,1	0.71 18	1.56 39,7	0.87 22,2	0.02 0,6		4 390 19,5	2 520 11,2	110 0,475	6 300	0.76 0,34	<b>YAR 206-102-2F</b>	
<b>1 <math>\frac{3}{16}</math></b> 30,163	2,4409 62	1.50 38,1	0.71 18	1.56 39,7	0.87 22,2	0.02 0,6		4 390 19,5	2 520 11,2	110 0,475	6 300	0.68 0,31	<b>YAR 206-103-2F</b>	
	2,4409 62	1.50 38,1	0.71 18	1.56 39,7	0.87 22,2	0.02 0,6		4 390 19,5	2 520 11,2	110 0,475	6 300	0.68 0,31	<b>YAR 206-103-2F/AH</b>	
	2,4409 62	1.22 31	0.71 18	1.56 39,7	0.87 22	0.04 1		4 390 19,5	2 520 11,2	110 0,475	6 300	0.62 0,28	<b>YAT 206-103</b>	
	2,4409 62	1.5 38,1	0.71 18	1.56 39,7	0.87 22,2	0.02 0,6		3 670 16,3	2 520 11,2	110 0,475	3 800	0.64 0,29	<b>YAR 206-103-2RF/HV</b>	
	2,4409 62	1.50 38,1	0.71 18	1.56 39,7	0.87 22,2	0.02 0,6		4 390 19,5	2 520 11,2	110 0,475	6 300	0.62 0,28	<b>YAR 206-104-2F</b>	
	2,8346 72	1.69 42,9	0.75 19	1.82 46,1	1.00 25,4	0.04 1		5 740 25,5	3 440 15,3	150 0,655	5 300	1.15 0,52	<b>YAR 207-104-2F</b>	
<b>1 <math>\frac{1}{4}</math></b> 31,75	2,8346 72	1.69 42,9	0.75 19	1.82 46,1	1.00 25,4	0.04 1		5 740 25,5	3 440 15,3	150 0,655	3 200	1.00 0,46	<b>YAR 207-104-2RF</b>	
	2,8346 72	1.69 42,9	0.75 19	1.82 46,1	1.00 25,4	0.04 1		4 860 21,6	3 440 15,3	150 0,655	3 800	1.15 0,52	<b>YAR 207-104-2RF/HV</b>	
	2,4409 62	1.22 31	0.71 18	1.56 39,7	0.87 22	0.04 1		4 390 19,5	2 520 11,2	110 0,475	6 300	0.61 0,28	<b>YAT 206-104</b>	
	2,8346 72	1.69 42,9	0.75 19	1.82 46,1	1.00 25,4	0.04 1		5 740 25,5	3 440 15,3	150 0,655	5 300	1.05 0,48	<b>YAR 207-105-2F</b>	
	2,8346 72	1.69 42,9	0.75 19	1.82 46,1	1.00 25,4	0.04 1		5 740 25,5	3 440 15,3	150 0,655	3 800	0.93 0,42	<b>YAR 207-106-2F/HV</b>	
	2,8346 72	1.69 42,9	0.75 19	1.82 46,1	1.00 25,4	0.04 1		5 740 25,5	3 440 15,3	150 0,655	5 300	1.00 0,46	<b>YAR 207-106-2RF</b>	
<b>1 <math>\frac{5}{16}</math></b> 33,338	2,8346 72	1.69 42,9	0.75 19	1.82 46,1	1.00 25,4	0.04 1		5 740 25,5	3 440 15,3	150 0,655	5 300	1.05 0,48	<b>YAR 207-105-2F</b>	
<b>1 <math>\frac{3}{8}</math></b> 34,925	2,8346 72	1.69 42,9	0.75 19	1.82 46,1	1.00 25,4	0.04 1		5 740 25,5	3 440 15,3	150 0,655	5 300	1.00 0,46	<b>YAR 207-106-2F</b>	
	2,8346 72	1.69 42,9	0.75 19	1.81 46,1	1 25,4	0.04 1		4 860 21,6	3 440 15,3	150 0,655	3 800	0.93 0,42	<b>YAR 207-106-2RF/HV</b>	
	2,8346 72	1.69 42,9	0.75 19	1.82 46,1	1.00 25,4	0.04 1		5 740 25,5	3 440 15,3	150 0,655	5 300	1.00 0,46	<b>YAR 207-107-2F</b>	
<b>1 <math>\frac{7}{16}</math></b> 36,513	2,8346 72	1.69 42,9	0.75 19	1.82 46,1	1.00 25,4	0.04 1		5 740 25,5	3 440 15,3	150 0,655	5 300	0.93 0,42	<b>YAR 207-107-2F</b>	
	2,8346 72	1.69 42,9	0.75 19	1.82 46,1	1.00 25,4	0.04 1		4 860 21,6	3 440 15,3	150 0,655	3 800	0.95 0,43	<b>YAR 207-107-2RF/HV</b>	
	3,1496 80	1.94 49,2	0.83 21	2,04 51,8	1,19 30,2	0.04 1		6 910 30,7	4 280 19	180 0,8	4 800	1.55 0.70	<b>YAR 208-107-2F</b>	
	2,8346 72	1.38 35	0.75 19	1.82 46,1	1.00 25,5	0.04 1		5 740 25,5	3 440 15,3	150 0,655	5 300	0.83 0,38	<b>YAT 207-107</b>	
	2,8346 72	1.38 35	0.75 19	1.82 46,1	1.00 25,5	0.04 1		5 740 25,5	3 440 15,3	150 0,655	5 300	0.83 0,38	<b>YAR 207-107</b>	
	2,8346 72	1.38 35	0.75 19	1.82 46,1	1.00 25,5	0.04 1		5 740 25,5	3 440 15,3	150 0,655	5 300	0.83 0,38	<b>YAR 207-107</b>	

## Bearing Analysis Calculations

From Catalogue:

For : SKF -YAR 206-104-2F

$$C = 19.5 \text{ kN}$$

$$C_D = 11.2 \text{ kN}$$

Applied Axial Load  $P = 5\text{DN}$

Assume → Due to weight of dust cover  
& spring force of housing (out of scope)

$$P < 0.02C (= 390) \\ \text{Very Light Load}$$

$$n = 196.9 \text{ rPM}$$

Max Lowering Speed

$$\text{Limiting speed } n_{max} = 6300 \text{ rPM}$$

$$L_{10} = \left(\frac{C}{P}\right)^3 = \left(\frac{19.5 \times 10^3}{5D}\right)^3 = 59.319 \text{ million cycles}$$

$$L_{10h} = \frac{10^6}{60n} \cdot L_{10} \\ = \frac{10^6 \times 59.319}{60 \times 196.9} \\ = 5.021 \times 10^9 \text{ hours}$$

Theoretically infinite life ✓

Static check

$$S_0 = \frac{C_0}{P_0} = \frac{11.2 \times 10^3}{0.5 \times D} = 448 \quad \checkmark$$

Speed Check

$$\text{Speed Factor} = \frac{n}{n_{max}} = \frac{196.9}{6300} = 0.0312$$

∴ Speed is ≈ 3% of rated speed ✓

$L_{10}$  = basic rating life (at 90% reliability), millions of revolutions

$L_{10h}$  = basic rating life (at 90% reliability), operating hours

C = basic dynamic load rating, kN

P = equivalent dynamic bearing load, kN

n = rotational speed, r/min

For bearings that accommodate axial loads only:

- $P = F_a$

$P \leq 0.02 C$  – very light load

$0.02 C < P \leq 0.035 C$  – light load

$0.035 C < P \leq 0.05 C$  – moderate load

$0.05 C < P \leq 0.1 C$  – normal load

$P > 0.1 C$  – heavy load

To select a Y-bearing or a Y-bearing unit size, the basic rating life is typically calculated in accordance with ISO 281:2007. The equation for ball bearings is

$$L_{10} = \left(\frac{C}{P}\right)^3$$

$$L_{10h} = \frac{1000000}{60n} L_{10}$$

$$P_0 = 0.6 F_r + 0.5 F_a$$

The requisite basic static load rating  $C_0$  can be determined from

$$C_0 = S_0 P_0$$

## 7.4. Ball Joint

Calculations:

$$F_{weight} = m_{system} \cdot g_{moon} \cdot SF = 30 \cdot 1.62 \cdot 1.4 = 68.04 N$$

$$D_{ball} = 1.6 \cdot D_{neck} \approx 30mm$$

$$\text{Ball expansion: } \delta d_{ball} = d_{ball} * \alpha * \delta T = 30 * \alpha * 80 = 0.055 mm$$

$$\text{Socket contraction: } \delta d_{socket} = d_{socket} * \alpha * \delta T = 30 * \alpha * -220 = -1.2 mm$$

$$\text{Total thermal displacement: } \delta d_{total} = 0.055 + 1.2 = 0.175mm$$

$$D_{open} > D_{neck} + 2[(R_{ball} \cdot \sin(\theta)) + C] = 23.5 mm$$

$$\text{Retention Overlap: } Overlap = \frac{D_{ball}-D_{open}}{2} = 3.25mm$$

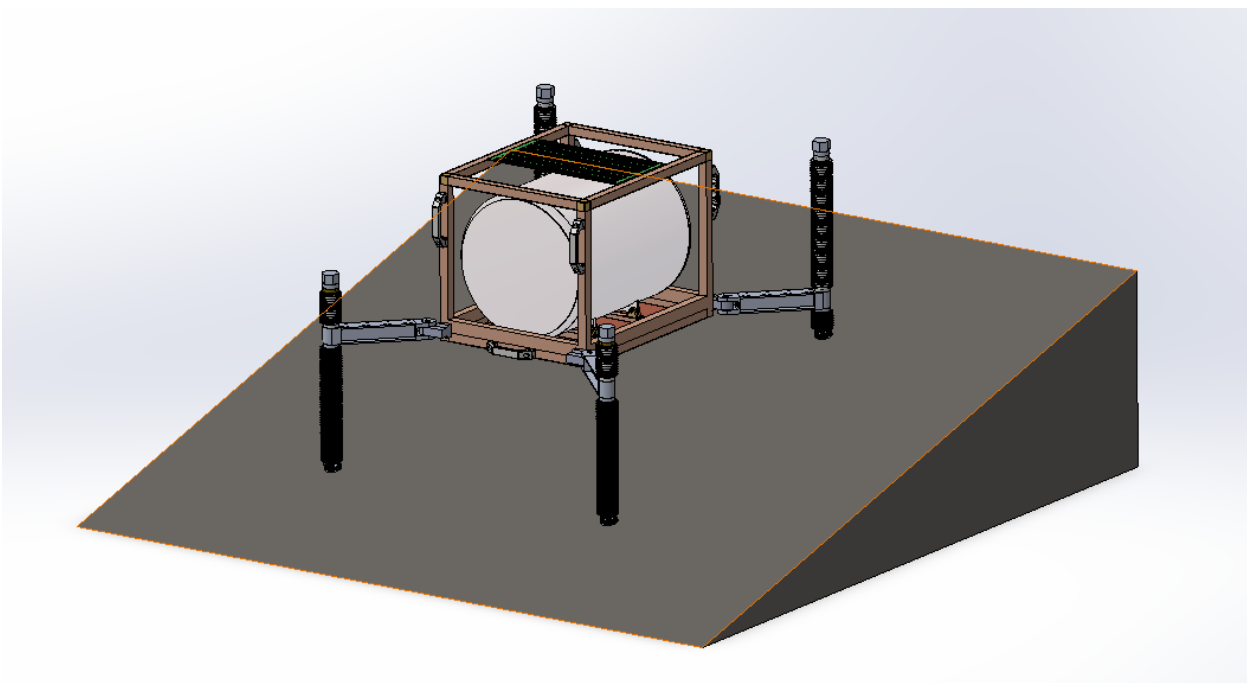
$$\text{Compressive failure load: } F_{fail} = \pi * r_{neck}^2 * \sigma_{yield} = 89kN$$

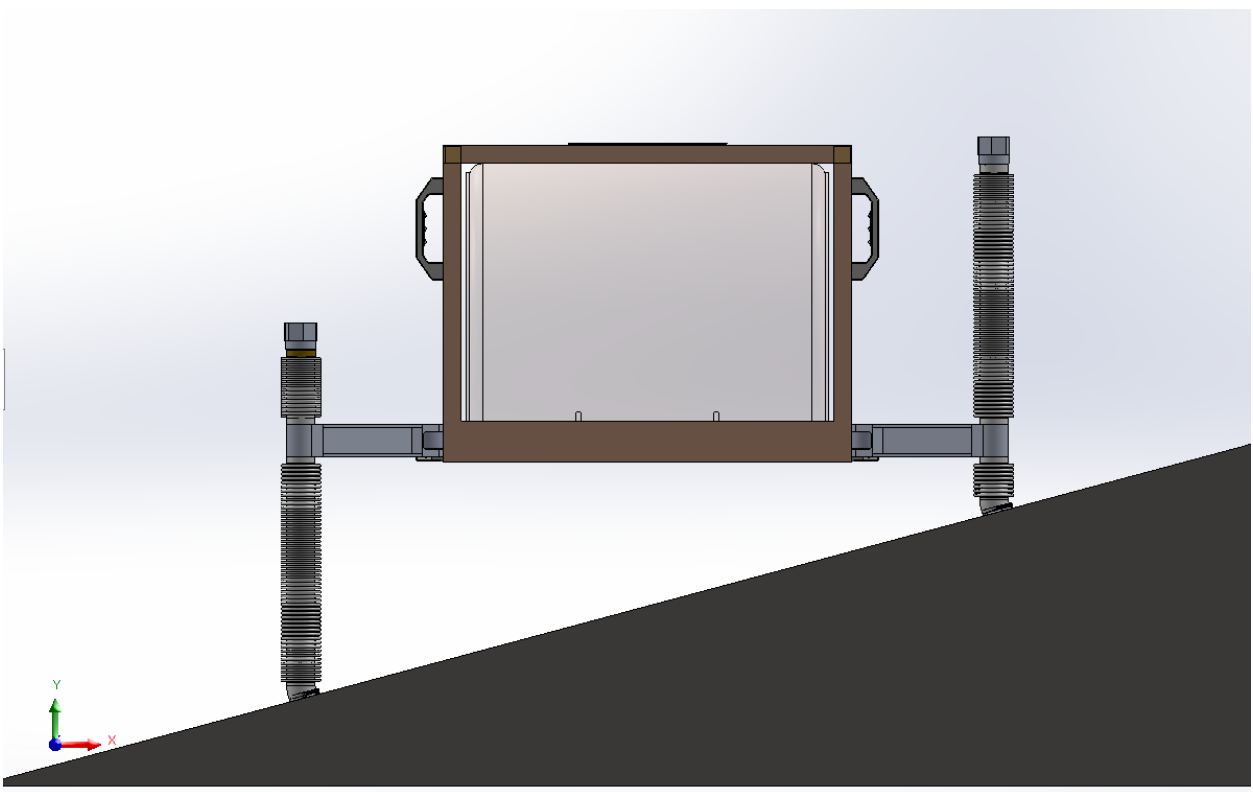
$$\text{Neck shear failure load: } F_{shear} = Overlap * \pi * d_{open} * \tau_{yield} \approx 48kN$$

$$\text{Neck shear stress: } \tau = \frac{F_{load} * \sin(15)}{\pi * r_{neck}^2} = 0.069 MPa \ll 200 = \tau_{yield}$$

## 7.5. Stability

The following calculations approximate the stability of the system when levelled on a slope of 15° incline. It is assumed that the reaction force at one end is zero in the moment just prior to tipping over, and the analysis is done in 2D. First with the long side of the OASYS body oriented uphill, and then with the short side oriented uphill. A sum of moments calculation is used to determine what force would be necessary to apply at the top edge of OASYS, acting in a perfect line, in order to cause the system to tip. The CAD model images illustrate this scenario:





Stability Calculation in 2D with short end oriented up hill and system levelled:

$$D_1 = \frac{850m}{2} \cos \left( \tan^{-1} \frac{550m}{850m} \right) + \frac{850mm - (850mm)(0.2)}{2}$$

$$= 696.81731679mm$$

$$D_2 = 1000mm$$

$$\textcircled{+} \sum M_P = 0$$

$$\rightarrow F_{\text{applied}} D_2 - M_{OASYS} G_{\text{Moon}} D_1 = 0$$

$$F_{\text{applied}}(1.0m) - (1.62 \frac{m}{s^2})(130kg)(0.69681731679m) = 0$$

$$\rightarrow F_{\text{applied}} = \frac{(1.62 \frac{m}{s^2})(130kg)(0.69681731679m)}{1.0m}$$

$$= 146.74972692N$$

Stability Calculation in 2D with long end oriented up hill and system levelled:

$$D_1 = \frac{850m}{2} \sin \left( \tan^{-1} \frac{550m}{850m} \right) + \frac{550mm - (550mm)(0.2)}{2}$$

$$= 560.88179322mm$$

$$D_2 = 1000mm$$

$$\textcircled{+} \sum M_P = 0$$

$$\rightarrow F_{\text{applied}} D_2 - M_{OASYS} G_{\text{Moon}} D_1 = 0$$

$$F_{\text{applied}}(1.0m) - (1.62 \frac{m}{s^2})(130kg)(0.56088179322m) = 0$$

$$\rightarrow F_{\text{applied}} = \frac{(1.62 \frac{m}{s^2})(130kg)(0.56088179322m)}{1.0m}$$

$$= 118.12170565N$$

## 7.6. Optimal Angle

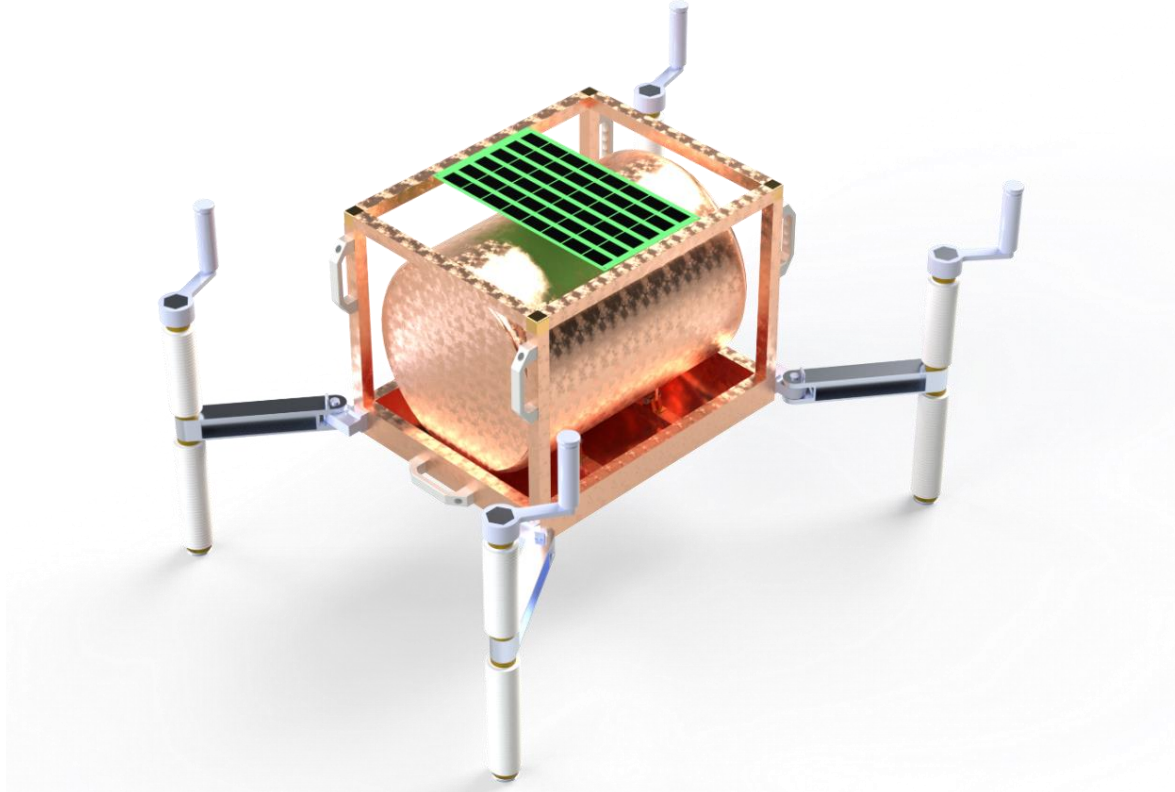
OASYS will be the most stable when the footprint of the deployed legs matches that of the main body (i.e. a rectangle with the same ratio of length to width when viewed from above). The angle that the hinged stabilizer beams would make with the long side of the OASYS body in such a case was determined using the length and width dimensions of OASYS as follows:

$$\theta_{\text{optimal}} = \tan^{-1} \left( \frac{550mm}{850mm} \right) = 32.90524292^\circ$$

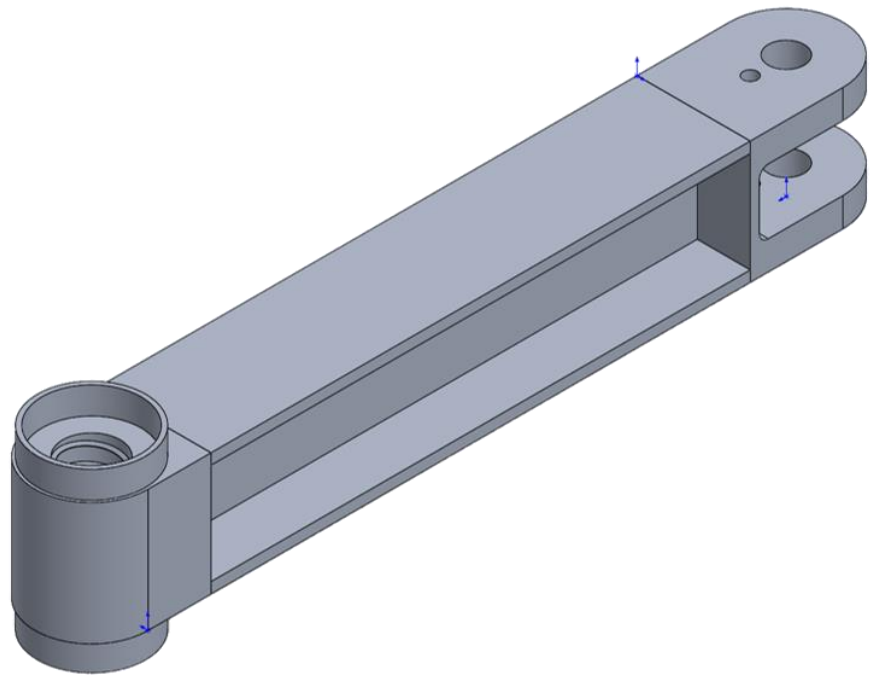
## **8. Appendix B – Extra CAD Figures**

### **8.1. Final Design (Integrated with full OASYS model)**

Note: crank assemblies are separate tools which slip over hex heads at top of shaft



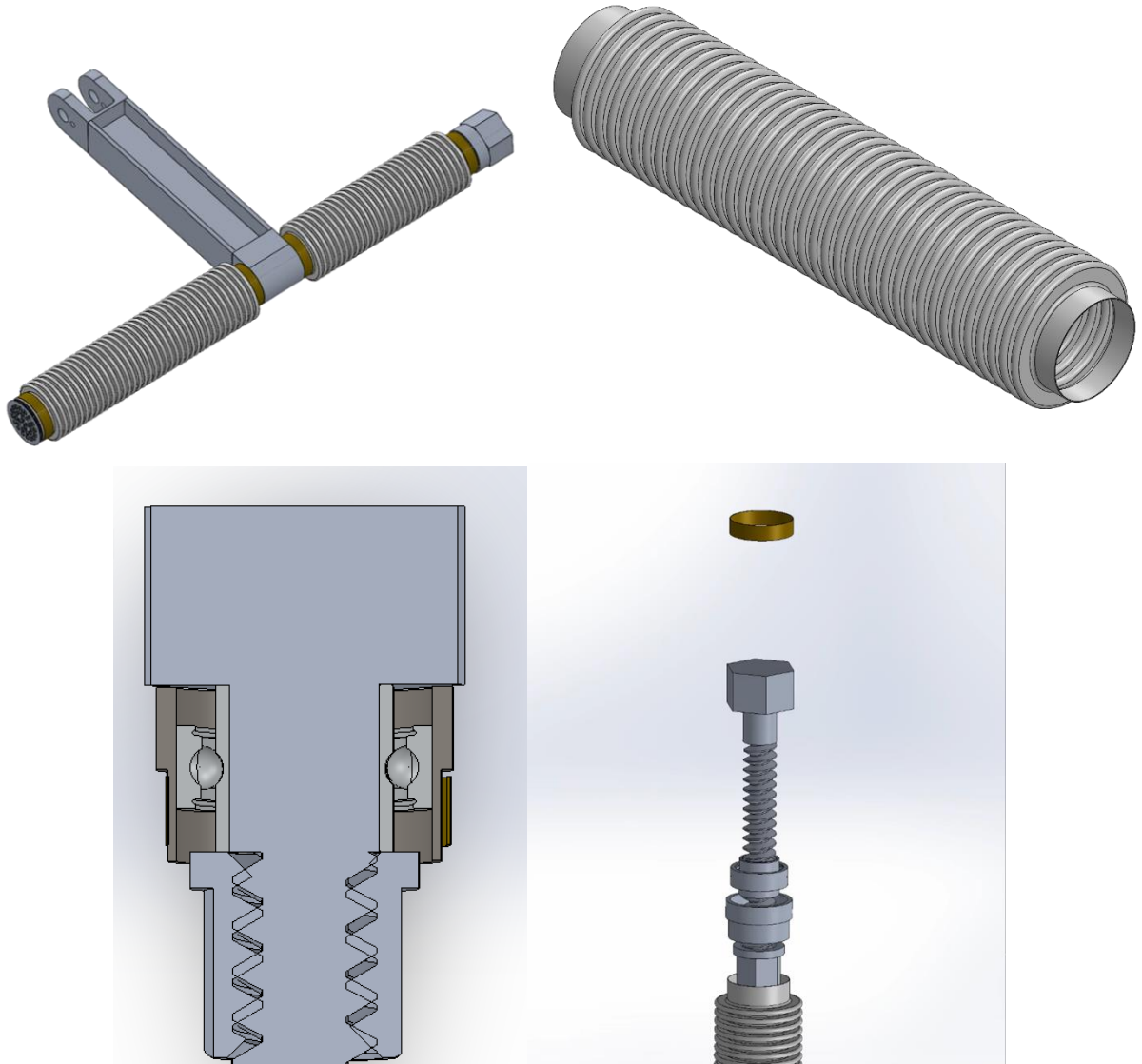
### **8.2. I-Beam**



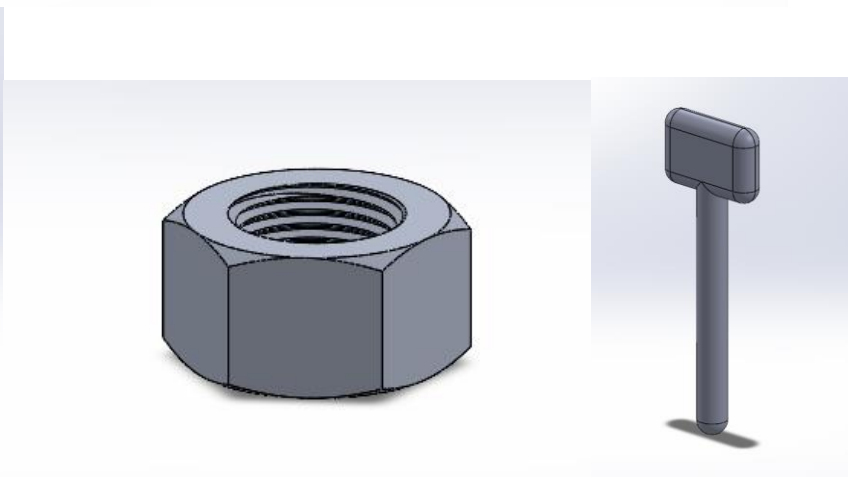
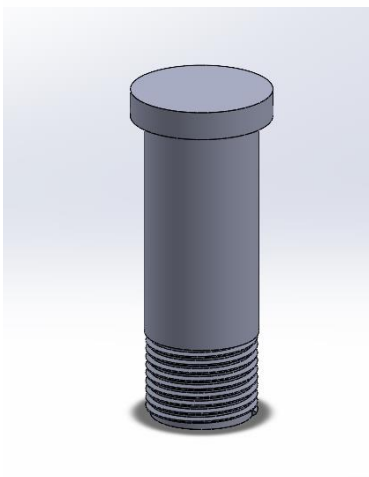
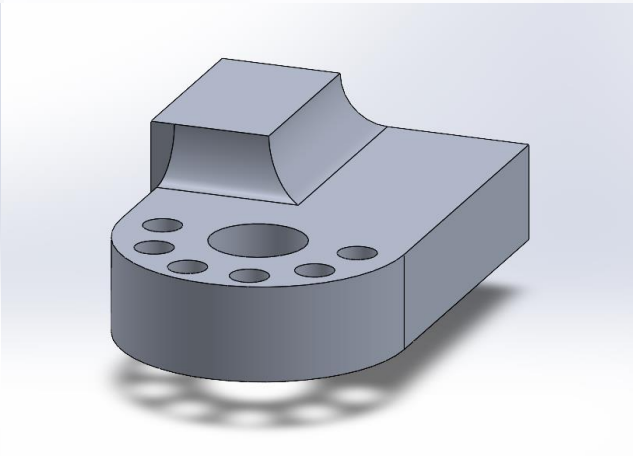
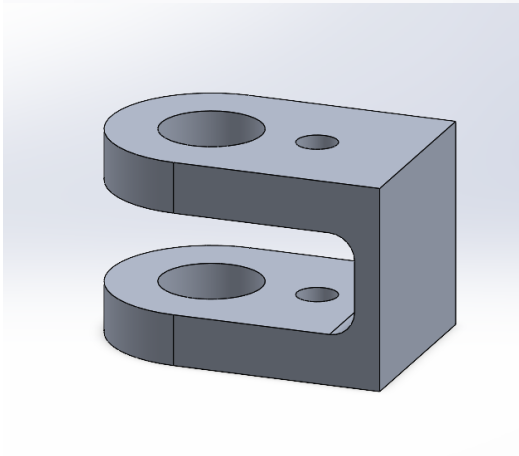
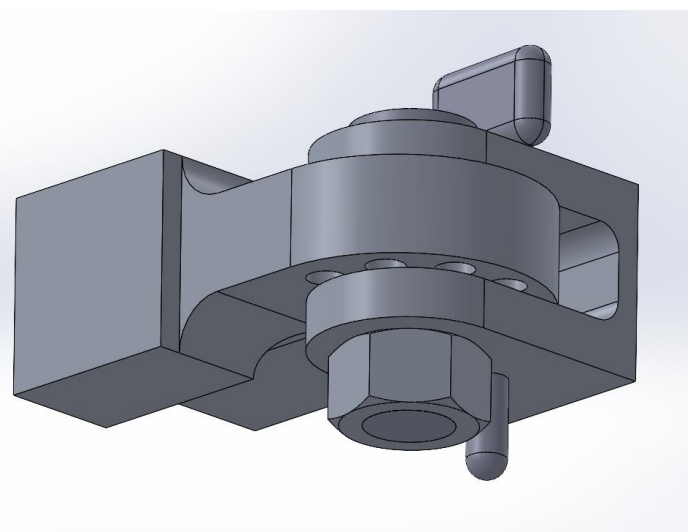
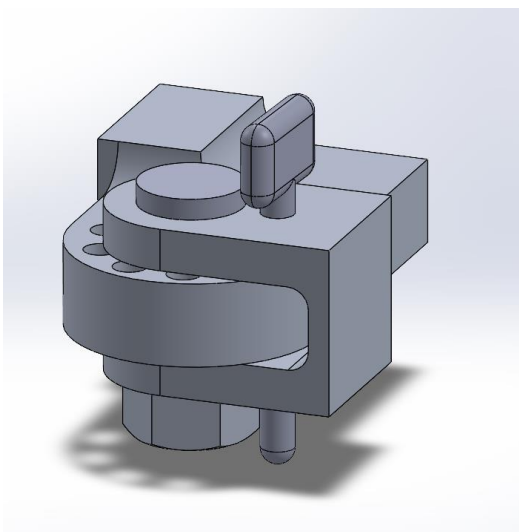
### 8.3. Lead Screw



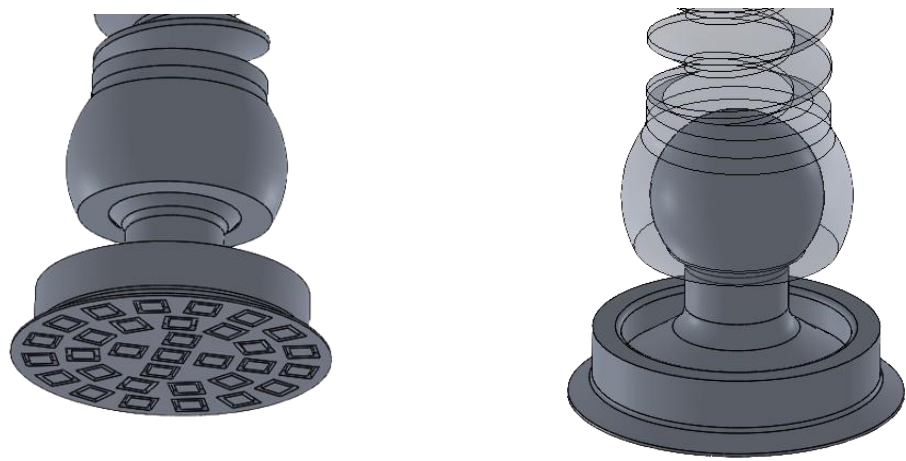
### 8.4. Dust Cover and Bearing



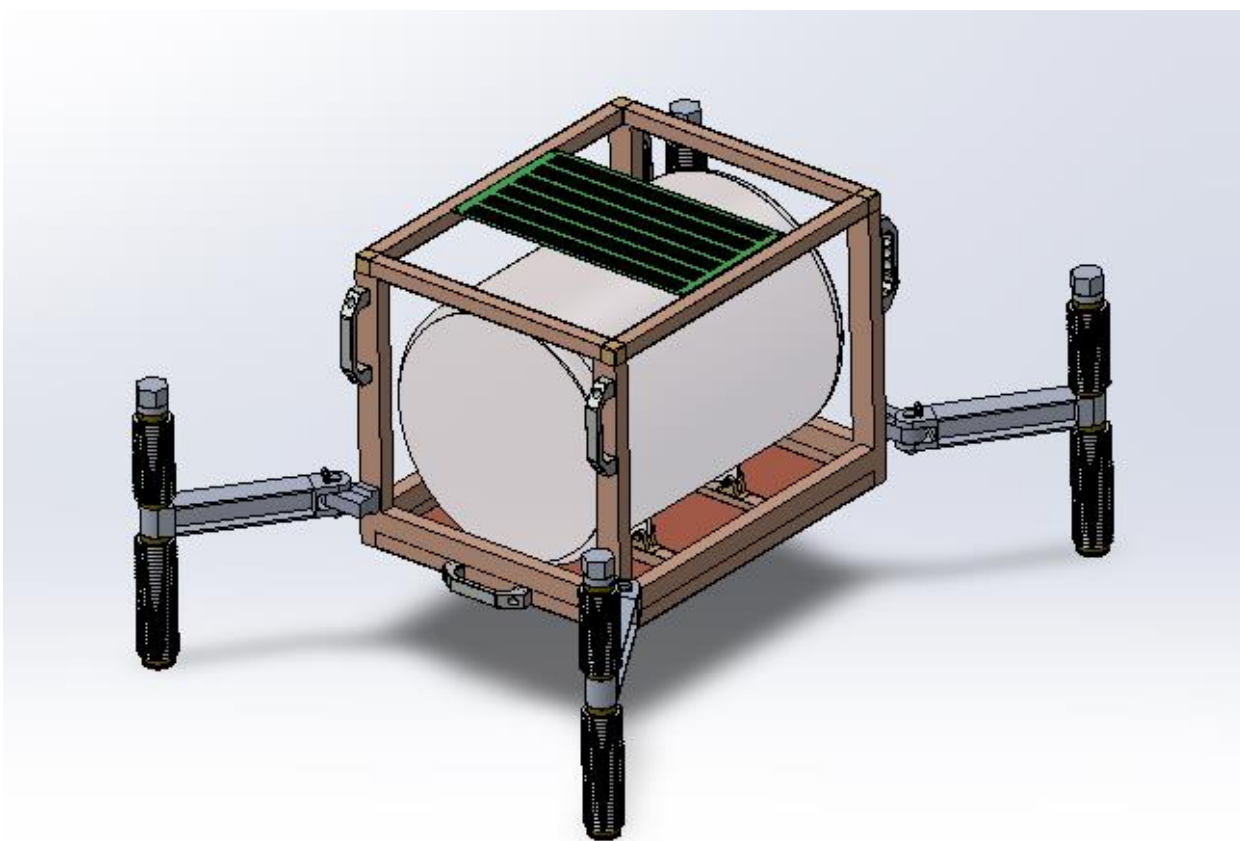
## 8.5. Hinge Mechanism



## 8.6. Ball Joint



### 8.7. Deployed View



### 8.8. Stowed View

